ELSEVIER

Comput. Methods Appl. Mech. Engrg. 132 (1996) 195–227

Computer methods in applied mechanics and engineering

A space–time finite element method for structural acoustics in infinite domains
Part 1: Formulation, stability and convergence

Lonny L. Thompson*, Peter M. Pinsky[1]

Department of Civil Engineering, Stanford University, Stanford, CA 94305-4020, USA

Received 24 August 1994; revised 14 September 1995

Abstract

A space–time finite element method for solution of the exterior structural acoustics problem involving the interaction of vibrating elastic structures submerged in an infinite acoustic fluid is formulated. In particular, time-discontinuous Galerkin and Galerkin Least-Squares (GLS) variational formulations for coupled structural acoustics in unbounded domains are developed and analyzed for stability and convergence. The formulation employs a finite computational fluid domain surrounding the structure and incorporates time-dependent non-reflecting boundary conditions on the fluid truncation boundary. Energy estimates are obtained which allow us to prove the unconditional stability of the method for the coupled fluid–structure problem with absorbing boundaries. The methods developed are especially useful for the application of adaptive solution strategies for transient acoustics in which unstructured space–time meshes are used to track waves propagating along space–time characteristics. An important feature of the space–time formulation is the incorporation of temporal jump operators which allow for finite element interpolations that are discontinuous in time. For additional stability, least-squares operators based on local residuals of the structural acoustics equations including the non-reflecting boundary conditions are incorporated. The energy decay estimates and high-order accuracy predicted by our a priori error estimates are demonstrated numerically in a simple canonical example.

1. Introduction

In this paper a space–time finite element method based on a new time-discontinuous Galerkin variational formulation for the coupled structural acoustics problem in infinite domains is presented. In this approach, the concept of space–time slabs is employed which allows for discretizations that are discontinuous in time. The order of accuracy of the solution is related to the order of the finite element spatial and temporal basis functions, and can be specified to any accuracy and for general unstructured discretizations within a space–time slab. The proposed space–time finite element formulation provides a powerful framework for simultaneous spatial and temporal discretization for transient structural acoustics. This is especially useful in the application of self-adaptive solution strategies, in which both spatial and temporal enhancement can be employed to efficiently track transient waves propagating along space–time characteristics in complicated fluid–structure interaction applications. In regions where the solution is smooth, the mesh can be relatively coarse while a finer mesh can be employed

* Corresponding author. Assistant Professor of Mechanical Engineering and Engineering Mechanics, Clemson University, Clemson, SC 29634-0921, USA.

[1] Associate Professor.

SSDI 0045-7825(95)00955-8

near wave fronts. Thus, an accurate solution may be obtained without resorting to a uniformly refined (and computationally expensive) mesh. Furthermore, the use of space–time *hp*-adaptive discretization strategies, where a combination of mesh size refinement/unrefinement (*h*-adaptivity), and finite element basis enrichment (*p*-adaptivity), can easily be accommodated in both space and time dimensions. In addition to these advantages, the resulting space–time algorithm possesses beneficial numerical filtering needed to resolve any steep gradients in the transient response and leads to stable higher-order accurate methods. An important property of the proposed time-discontinuous approach for structural acoustics in infinite domains is that it allows for the implementation of high-order accurate non-reflecting boundary conditions involving high-order temporal derivatives in a simple and straightforward manner.

Considerable progress has been made in the development of stabilized space–time finite element methods based on a time-discontinuous Galerkin formulation for problems that can be written as a system of first-order equations (see e.g. [1–5]). Classical linear acoustics equations can be converted to first-order hyperbolic form and these methods are thus immediately applicable. However, in this approach, the coupled state vector consists of fluid pressure and velocity components, which is computationally uneconomical.

A direct approach is to develop space–time finite element methods for structural acoustics based on the natural framework of second-order hyperbolic equations for elastodynamics and the acoustic wave equation. Recently, Hughes and Hulbert [6] and Hulbert and Hughes [7] have successfully generalized time-discontinuous space–time finite element methods developed for first-order systems to the second-order hyperbolic equations of elastodynamics. In this paper, the space–time formulation is extended to include both the elastic structure and acoustic fluid posed in second-order hyperbolic form together with their interaction. Throughout the development, a priori energy estimates for the continuum problem are used as a guide for the design of the proposed space–time algorithms. The formulation employs a finite computational fluid domain surrounding the structure and incorporates high-order accurate radiation (non-reflecting) boundary conditions on the fluid truncation boundary. Non-reflecting boundary conditions are incorporated as 'natural' boundary conditions in the space–time variational equation, i.e. they are enforced weakly in both space and time. For the coupled equations, scalar velocity potential ϕ is used as the solution variable for the acoustic fluid, while the displacement vector $\boldsymbol{u}$ is used as the primary variable for the structure. As a consequence of this choice of variables, the coupled variational equations for the fluid and structure gives rise to a positive form, which enables us to prove the unconditional stability of the space–time finite element formulation.

An important ingredient for the success of the proposed space–time finite element method is the incorporation of time-discontinuous jump operators that weakly enforce continuity of the solution between space–time slabs. The specific form of these temporal jump operators are designed such that unconditional stability can be proved a priori for general unstructured discretizations within a space–time slab. An algorithm is termed unconditionally stable if in the absence of forcing terms but for arbitrary initial conditions, the computed total structural acoustic energy plus the radiation energy absorbed through the artificial boundary is always less than or equal to the initial total energy for the system, for arbitrary step sizes.

For additional stability, and to prove convergence, least-squares operators based on local residuals of the Euler–Lagrange equations for the coupled system, including the non-reflecting boundary conditions, are incorporated into the space–time formulation. Stabilized methods of this type are referred to as Galerkin Least-Squares (GLS) methods. GLS methods were originally developed to improve the stability of numerical solutions for the advection–diffusion equation [8], and the Euler and Navier–Stokes equations [3]. These ideas have since been extended to other applications requiring improved stability and/or accuracy; e.g. the reduced wave equation for time-harmonic wave propagation in [9–12], steady advection–diffusion with production [13], and to second-order hyperbolic equations in the context of elastodynamics in [6, 7]. In this paper, we extend the idea of GLS stabilization to the coupled fluid–structure interaction problem for transient structural acoustics including the incorporation of fluid–structure interaction and non-reflecting boundaries.

Previous approaches to the transient structural acoustics problem involving the interaction of vibrating structures submerged in an infinite acoustic fluid have employed: (i) boundary element

methods based on Kirchhoff's retarded potential integral formulation (see e.g. [14–16]), (ii) semi-discrete finite element methods which employ finite difference techniques for integrating in time (also referred to as the method of lines) (see e.g. [17, 18]), and (iii) Taylor–Galerkin methods (e.g. [19]). Semi-discrete finite element methods developed within the context of structural dynamics, e.g. [20, 21], HHT-α algorithms will generally not adequately capture all the important solution features appearing in physically realistic transient structural acoustics applications. Other difficulties include the incorporation of high-order accurate absorbing boundary conditions and truly self-adaptive schemes in a semidiscrete finite element formulation for transient wave propagation in infinite domains. The difficulties and limitations of standard computational methods for structural acoustics have motivated the development of the new space–time finite element formulation proposed in this work.

In Section 2 the coupled system for the exterior structural acoustics problem is described where the governing differential equations for the structure, the acoustic fluid and their interaction are summarized. In Section 3 a number of important a priori energy estimates for the continuum problem are established. These results play a central role in the analysis of stability for both the continuum and discrete problems and form the basis for the design of the new time-discontinuous Galerkin variational formulation proposed in this paper. In Section 4 the space–time finite element method for the coupled structural acoustics problem is formulated. Galerkin Least-Squares stabilization is discussed in Section 5. In Section 7 an analysis of the coupled space–time variational formulation is performed where the unconditional stability and convergence of the method is established. Energy estimates and convergence rates are demonstrated numerically with a one-dimensional canonical example. Conclusions and extensions are given in Section 10.

2. Governing equations for structural acoustics

In this work, the exterior structural acoustics problem involving solution of the coupled wave equation defined over an infinite domain is transformed to a coupled fluid–structure interaction problem defined over a finite computational domain through the introduction of an artificial fluid truncation boundary. Radiation boundary conditions are prescribed on the fluid truncation boundary in the form of a linear operator which approximates the asymptotic behavior of the solution at infinity.

The coupled fluid–structure system is illustrated in Fig. 1, and consists of the artificial truncation boundary Γ_∞ enclosing a finite computational domain Ω. The finite computational domain is composed of the fluid domain Ω_f, which in turn surrounds the structural domain Ω_s such that $\Omega = \Omega_f \cup \Omega_s$. The fluid boundary $\partial\Omega_f$, is divided into the fluid–structure interface boundary Γ_i and the artificial boundary Γ_∞. The structural boundary $\partial\Omega_s$, is composed of the shared fluid–structure interface boundary Γ_i and a traction boundary Γ_σ. The infinite domain outside the artificial boundary and extending to infinity is denoted by Ω_∞. The fluid is assumed to be homogeneous in Ω_∞, but may be inhomogeneous within Ω_f.

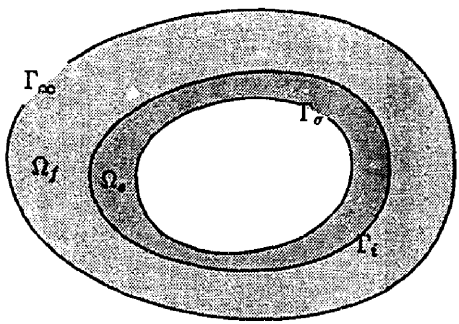

Fig. 1. Coupled system for the exterior fluid–structure interaction problem, with artificial boundary Γ_∞ enclosing the finite computational domain $\Omega = \Omega_f \cup \Omega_s$.

The domain interior to the elastic body is assumed to be in vacuo, although the inclusion of an interior fluid can be accommodated with no special difficulty. The density of the fluid is assumed comparable to the inertial and elastic forces in the structure so that significant interaction exists. In the following, the equations governing the structure, the acoustic fluid and their interaction are summarized.

The governing equations for the structure are stated for a linear solid continuum without the explicit imposition of kinematic constraints common to structural models such as plates and shells. In this way, full generality of the formulation is maintained in order to accommodate a wide class of shell models into the formulation. Consider an elastic body occupying the bounded domain $\Omega_s \subset \mathbb{R}^d$, where $d = 1, 2$ or 3 is the number of space dimensions. The structural displacement vector is denoted by $\boldsymbol{u}(\boldsymbol{x}, t)$, where $\boldsymbol{x} \in \Omega_s$ and $t \in I =]0, T[$, is the time interval of interest of length $T > 0$. The equations of motion for the structure are governed by the linear momentum balance,

$$\nabla \cdot \boldsymbol{\sigma} = \rho_s \ddot{\boldsymbol{u}} \quad \text{in } Q_s := \Omega_s \times]0, T[\tag{1}$$

where $\rho_s = \rho_s(\boldsymbol{x}) > 0$ is the structural density, a superposed dot indicates partial differentiation with respect to time t, and $\boldsymbol{\sigma}$ is the symmetric Cauchy stress tensor which is related to the displacements through the constitutive equation,

$$\boldsymbol{\sigma} = \boldsymbol{C} : \varepsilon[\boldsymbol{u}] \tag{2}$$

In this expression, the strain tensor is denoted by $\varepsilon[\boldsymbol{u}] = \nabla^s \boldsymbol{u}$, where $\nabla^s \boldsymbol{u}$ is the symmetric gradient of the displacement vector. The elastic coefficients $\boldsymbol{C} = \boldsymbol{C}(\boldsymbol{x})$ are assumed to satisfy the usual positive-definiteness (pointwise stability) and major and minor symmetry assumptions for an elastic solid continuum.

With Γ_σ and Γ_i denoting non-overlapping subregions of $\partial\Omega_s$ such that $\partial\Omega_s = \overline{\Gamma_\sigma \cup \Gamma_i}$, prescribed tractions $\bar{\boldsymbol{t}}$, are enforced through the boundary condition,

$$\boldsymbol{\sigma} \cdot \boldsymbol{n} = \bar{\boldsymbol{t}} \quad \text{on } Y_\sigma := \Gamma_\sigma \times]0, T[\tag{3}$$

The specification of coupling conditions on the structure–fluid interface Γ_i are discussed later in this section. Here, we note that two interface conditions are required: (i) a kinematic interface condition, and (ii) a traction interface condition.

The acoustic fluid is modeled under the usual assumptions governing the linearized theory of sound. Under the standard acoustic approximation, the motion of an inviscid, irrotational and compressible fluid is regarded as a small perturbation from a uniform reference state. Linearizing the conservation equations of compressible inviscid flow around a reference state in which the fluid has a uniform density ρ_0 and is at rest, and with products of small quantities neglected, the equations of momentum and of continuity for the acoustic fluid take the form (see e.g. [22]):

$$\rho_0 \dot{\boldsymbol{v}} + \nabla p = 0 \tag{4}$$

$$\dot{p} + \rho_0 c^2 \nabla \cdot \boldsymbol{v} = 0 \tag{5}$$

where p and $\boldsymbol{v}$ denote perturbations of pressure and velocity from the reference state. The relationship between changes in pressure and density are given by the linearized equation of state, $\dot{p} = c^2 \dot{\rho}$, where $c > 0$ is the speed of sound.

Defining a state vector as

$$\boldsymbol{U} = (p, v_1, v_2, v_3)^{\mathrm{T}} \tag{6}$$

where v_i are the velocity components in $\mathbb{R}^3$, these equations can be arranged in standard first-order hyperbolic form as

$$\frac{\partial \boldsymbol{U}}{\partial t} + \sum_{i=1}^{3} \boldsymbol{A}_i \frac{\partial \boldsymbol{U}}{\partial x_i} = 0 \tag{7}$$

and $\boldsymbol{A}_i \in \mathbb{R}^{4\times 4}$, $i = 1, \ldots, 3$ are sparse unsymmetric matrices for the system in $\mathbb{R}^3$. Considerable progress has been made in the development of stabilized time-discontinuous Galerkin finite elements

methods for first-order hyperbolic and parabolic systems; see for example [1–3, 23] and references therein. These methods are immediately applicable to the classical linear acoustics equations written in the first-order form (7). However, in this approach, the state vector consists of both pressure and velocity components, requiring a large number of solution variables, which may be computationally uneconomical. Another difficulty with this approach is the coupling between the natural second-order form of the momentum equations governing the structure, and a first-order form for the system of equations describing the acoustic fluid. As a result of the mismatch between the second-order and first-order systems for the structure and fluid, respectively, rigorous stability and convergence proofs for the coupled fluid–structure system are difficult to obtain.

A natural approach for the coupled problem is to recast the first-order system of acoustic equations given in (7) as a second-order hyperbolic equation in terms of a single scalar variable. The most common choice is to eliminate the velocity in terms of the scalar pressure variable. Taking the divergence of (4) and the time derivative of (5), and after eliminating the velocity in terms of pressure the second-order scalar wave equation is obtained,

$$\nabla^2 p = a^2 \ddot{p} \tag{8}$$

where $a = c^{-1} > 0$ is the slowness and $\nabla^2 = \mathrm{Div}(\mathrm{Grad})$ is the Laplacian operator. Traditional variational (weak) formulations for the coupled structural acoustics problem are based on this second-order hyperbolic wave equation in terms of the scalar acoustic pressure p, together with the equations of elastodynamics in terms of the structural displacement $\boldsymbol{u}$, see e.g. [24] for this approach in the context of the semidiscrete finite element method. While this approach reduces the number of solution variables in the formulation, the use of $\{\boldsymbol{u}, p\}$ variables leads to an unsymmetric coupled system of equations for the fluid–structure problem. As a result of this lack of symmetry, stability and energy estimates for both the continuum and discrete structural-acoustic problems are difficult to obtain a priori.

To eliminate this difficulty for the coupled problem, the scalar velocity potential ϕ is chosen as the solution variable for the acoustic fluid, in conjunction with the displacement vector $\boldsymbol{u}$, for the structure. In the following discussions it will be shown that as a consequence of this choice of variables, the coupled variational equations associated with the fluid–structure interaction problem gives rise to a positive form. The positive form is essential for the proof of stability and convergence of the space–time finite element method.

The use of the velocity potential follows directly from the assumption of an irrotational acoustic fluid. For an irrotational fluid the acoustic velocity $\boldsymbol{v}$ can be written as the gradient of the velocity potential ϕ:

$$\boldsymbol{v} = \nabla\phi \tag{9}$$

Substituting (9) into (4) and (5) and eliminating the pressure in terms of the velocity potential $\phi(\boldsymbol{x}, t)$, results in the second-order hyperbolic wave equation,

$$\nabla^2\phi = a^2\ddot{\phi} \quad \text{in } Q_f := \Omega_f \times]0, T[\tag{10}$$

The unique solution to the coupled problem requires two interface conditions between the structure and fluid: (i) a traction boundary condition, and (ii) a kinematic compatability condition. The traction boundary condition represents the acoustic fluid pressure acting on the structure and is given by

$$\boldsymbol{\sigma}\cdot\boldsymbol{n} = -p\boldsymbol{n} \quad \text{on } Y_I := \Gamma_I \times]0, T[\tag{11}$$

where the acoustic pressure is related to the velocity potential through the equation of momentum for the fluid, $p = -\rho_0\dot{\phi}$ and $\boldsymbol{n}$ is the unit outward normal to Ω_s and inward normal to Ω_f, on Γ_I. The kinematic boundary condition provides for the compatibility of the normal velocity across the fluid–structure interface and is given by

$$\boldsymbol{v}\cdot\boldsymbol{n} = \dot{\boldsymbol{u}}\cdot\boldsymbol{n} \quad \text{on } Y_I := \Gamma_I \times]0, T[\tag{12}$$

where $\boldsymbol{v} = \nabla\phi$.

Non-reflecting boundary conditions are imposed on the artificial boundary Γ_∞ in the form of a linear operator $\mathbb{S}_m$, relating the velocity potential to the normal velocity on Γ_∞:

$$\boldsymbol{v}\cdot\boldsymbol{n} = -\mathbb{S}_m\phi \quad \text{on } Y_\infty := \Gamma_\infty \times]0, T[\tag{13}$$

This boundary condition approximates the asymptotic behavior of the solution at infinity as described by the Summerfeld condition, i.e.

$$\lim_{r\to\infty} r^{(d-1)/2}\left(\frac{\partial}{\partial r} + \frac{1}{c}\frac{\partial}{\partial t}\right)\phi = 0 \quad r + ct = \text{constant} \tag{14}$$

where r is the radial distance from the source and d is the number of spatial dimensions. This condition asserts that at infinity all waves are outgoing. The non-reflecting boundary condition (13) can take several different forms depending on the local (differential) or non-local (integral) operators appearing in $\mathbb{S}_m$. An example is given here for the first-order accurate boundary condition,

$$\boldsymbol{v}\cdot\boldsymbol{n} = -\mathbb{S}_1\phi\,, \quad \text{where } \mathbb{S}_1 := \frac{1}{R} + \frac{1}{c}\frac{\partial}{\partial t} \tag{15}$$

and $r = R$ is a fixed radius for a spherical truncation boundary Γ_∞. This radiation boundary condition is exact only for axially symmetric waves in $\mathbb{R}^3$. A number of high-order accurate non-reflecting boundary conditions which take the form of (13) are available, e.g. [25]. Here, we note that the index m, is related to the order of temporal derivatives appearing in the operator.

The strong form

After collecting the governing equations defined in the preceding sections, the strong (local) form of the fluid–structure initial/boundary-value problem may be stated as:
Given a prescribed traction $\bar{t}: \Gamma_\sigma \times I \mapsto \mathbb{R}^d$ and a source $f: \Omega_f \times I \mapsto \mathbb{R}$,
Find $\boldsymbol{u}: \Omega_s \times I \mapsto \mathbb{R}^d$ and $\phi: \Omega_f \times I \mapsto \mathbb{R}$, such that

$$\nabla\cdot\boldsymbol{\sigma} = \rho_s\ddot{\boldsymbol{u}} \quad \text{in } Q_s := \Omega_s \times I \tag{16}$$

$$\boldsymbol{\sigma} = \boldsymbol{C}:\nabla^s\boldsymbol{u} \quad \text{in } Q_s := \Omega_s \times I \tag{17}$$

$$\nabla^2\phi - a^2\ddot{\phi} = f \quad \text{in } Q_f := \Omega_f \times I \tag{18}$$

$$\boldsymbol{\sigma}\cdot\boldsymbol{n} = \bar{\boldsymbol{t}} \quad \text{on } Y_\sigma := \Gamma_\sigma \times I \tag{19}$$

$$\boldsymbol{\sigma}\cdot\boldsymbol{n} = \rho_0\dot{\phi}\boldsymbol{n} \quad \text{on } Y_i := \Gamma_i \times I \tag{20}$$

$$\nabla\phi\cdot\boldsymbol{n} = \dot{\boldsymbol{u}}\cdot\boldsymbol{n} \quad \text{on } Y_i := \Gamma_i \times I \tag{21}$$

$$\nabla\phi\cdot\boldsymbol{n} = -\mathbb{S}_m\phi \quad \text{on } Y_\infty := \Gamma_\infty \times I \tag{22}$$

with initial conditions,

$$\boldsymbol{u}(\boldsymbol{x}, 0) = \boldsymbol{u}_0(\boldsymbol{x}) \quad \text{for } \boldsymbol{x} \in \Omega_s \tag{23}$$

$$\dot{\boldsymbol{u}}(\boldsymbol{x}, 0) = \dot{\boldsymbol{u}}_0(\boldsymbol{x}) \quad \text{for } \boldsymbol{x} \in \Omega_s \tag{24}$$

$$\phi(\boldsymbol{x}, 0) = \phi_0(\boldsymbol{x}) \quad \text{for } \boldsymbol{x} \in \Omega_f \tag{25}$$

$$\dot{\phi}(\boldsymbol{x}, 0) = \dot{\phi}_0(\boldsymbol{x}) \quad \text{for } \boldsymbol{x} \in \Omega_f \tag{26}$$

Eqs. (16)–(22) together with the initial conditions define a linear coupled system of second-order hyperbolic type.

3. Energy estimates for the continuum problem

In this section we establish some a priori estimates for the continuum problem in terms of the energy for the hyperbolic structure–fluid coupled system using structural displacement $\boldsymbol{u}$ and acoustic velocity potential ϕ variables. The study of these important mathematical properties provides a general

framework for the design and stability analysis of the proposed space–time finite element formulation. Let the solution vector be defined in abstract form as

$$\chi := \{u, \phi\} \tag{27}$$

Then define the total energy for the coupled domain $\Omega = \Omega_s \cup \Omega_f$ by the expression,

$$\mathbb{E}(\chi) := \mathscr{E}_s(u) + \mathscr{E}_f(\phi) \tag{28}$$

where the total structural energy in terms of the structural displacements is

$$\mathscr{E}_s(u) := \frac{1}{2}\int_{\Omega_s} [\rho_s \dot{u}\cdot\dot{u} + \varepsilon(u) : C : \varepsilon(u)]\, d\Omega \tag{29}$$

and the acoustic energy or 'wave energy' in terms of the velocity potential is

$$\begin{aligned}\mathscr{E}_f(\phi) &:= \frac{1}{2}\int_{\Omega_f} \rho_0\left[\left(\frac{p}{\rho_0 c}\right)^2 + v\cdot v\right] d\Omega \\ &= \frac{1}{2}\int_{\Omega_f} \rho_0[a^2(\dot{\phi})^2 + \nabla\phi\cdot\nabla\phi]\, d\Omega\end{aligned} \tag{30}$$

The first and second terms in (29) are the kinetic and strain energy for the elastic structure, respectively. The form of the acoustic energy written in terms of velocity potential is in reverse order: the first term (time derivative squared) and second term (gradient squared) in (30) are the potential and kinetic energies, respectively. The total energy for the coupled system $\mathbb{E}(\chi)$ defines a natural energy norm on the space $\mathscr{V} = [H^1(\Omega_s)]^d \times H^1(\Omega_f)$, i.e. $\mathbb{E}(\chi) := \|\chi\|_{\mathscr{V}}^2$.

The acoustic intensity for sound waves is defined as the vector $I := pv$, where p and v are the acoustic pressure and velocity, respectively (see e.g. [26]). In terms of the velocity potential the acoustic intensity vector takes the form,

$$I = -\rho_0\dot{\phi}\nabla\phi \tag{31}$$

whose component $I\cdot n$ is the rate per unit area at which energy is transmitted in the direction of the unit normal n. For the exterior problem the rate of energy (power), $\mathscr{P}$, absorbed through the artificial boundary Γ_∞ is then,

$$\mathscr{P}(\phi) := -\int_{\Gamma_\infty} \rho_0\dot{\phi}\nabla\phi\cdot n\, d\Gamma \tag{32}$$

In terms of the absorbing boundary conditions defined through the linear map $\mathbb{S}_m$ given in (13),

$$\mathscr{P}(\phi) = \int_{\Gamma_\infty} \rho_0\dot{\phi}\mathbb{S}_m\phi\, d\Gamma \tag{33}$$

With these definitions in place, the following energy estimate for the coupled structural acoustics problem in exterior domains can be proved.

LEMMA 3.1 (Energy estimate). Under the conditions of zero sources $f = 0$ in Ω_f, and homogeneous traction boundary conditions $\bar{t} = 0$ on Γ_σ, then the time rate of change of structural acoustic energy in $\Omega = \Omega_s \cup \Omega_f$ is equal to the total rate of transport through the artificial boundary Γ_∞, i.e.

$$\frac{d}{dt}\mathbb{E}(\chi) = -\mathscr{P}(\phi), \quad \forall t \geq 0 \tag{34}$$

where $\chi = \{u, \phi\}$.

PROOF. The proof of this important result employs integration by parts and provides the key motivation for the space–time finite element formulation proposed in this paper. Computing the time derivative we have,

$$\frac{\mathrm{d}}{\mathrm{d}t}\mathscr{E}_s(\boldsymbol{u}) = \int_{\Omega_s} [\rho_s \dot{\boldsymbol{u}}\cdot\ddot{\boldsymbol{u}} + \boldsymbol{\varepsilon}(\dot{\boldsymbol{u}}):\boldsymbol{C}:\boldsymbol{\varepsilon}(\boldsymbol{u})]\,\mathrm{d}\Omega$$

$$= \int_{\Omega_s} [\dot{\boldsymbol{u}}\cdot(\nabla\cdot\boldsymbol{\sigma}) + \boldsymbol{\varepsilon}(\dot{\boldsymbol{u}}):\boldsymbol{C}:\boldsymbol{\varepsilon}(\boldsymbol{u})]\,\mathrm{d}\Omega$$

$$= \int_{\Gamma_i} \rho_0 \dot{\phi}\dot{\boldsymbol{u}}\cdot\boldsymbol{n}\,\mathrm{d}\Gamma \tag{35}$$

Similarly,

$$\frac{\mathrm{d}}{\mathrm{d}t}\mathscr{E}_f(\phi) = \int_{\Omega_f} \rho_0[a^2\dot{\phi}\ddot{\phi} + \nabla\dot{\phi}\cdot\nabla\phi]\,\mathrm{d}\Omega$$

$$= \int_{\Omega_f} \rho_0[\dot{\phi}\nabla^2\phi + \nabla\dot{\phi}\cdot\nabla\phi]\,\mathrm{d}\Omega$$

$$= -\int_{\Gamma_i} \rho_0\dot{\phi}\dot{\boldsymbol{u}}\cdot\boldsymbol{n}\,\mathrm{d}\Gamma - \int_{\Gamma_\infty} \rho_0\dot{\phi}\mathbb{S}_m\phi\,\mathrm{d}\Gamma \tag{36}$$

Combining (35) and (36) gives the desired energy estimate (34). □

REMARK. It is important to note that by choosing the velocity potential ϕ for the acoustic variable and enforcing the compatibility of normal velocity (12) across Γ_i, then the coupling integrals defined on the fluid–structure interface boundary Γ_i, cancel when (35) and (36) are added together to form (34). This is the key property associated with the choice of χ variables and plays an important role in the stability (energy) estimates for the space–time formulation.

THEOREM 3.1 (Energy identity). At any given time $t>0$, the energy in $\Omega = \Omega_s \cup \Omega_f$ plus the energy absorbed through the artificial boundary Γ_∞ is equal to the initial energy in the coupled system, i.e.

$$\mathscr{E}_s(\boldsymbol{u}(t)) + \mathscr{E}_f(\phi(t)) + \mathscr{R}(\phi(t)) = \mathscr{E}_s(\boldsymbol{u}_0) + \mathscr{E}_f(\phi_0)\,, \quad \forall\, t \geq 0 \tag{37}$$

where

$$\mathscr{R}(\phi(t)) := \int_0^t \mathscr{D}(\phi(\tau))\,\mathrm{d}\tau \tag{38}$$

is the radiation energy.

PROOF. Integrating (34) over time,

$$\mathbb{E}(\boldsymbol{\chi})\big|_0^t + \int_0^t \mathscr{D}(\phi(\tau))\,\mathrm{d}\tau = 0 \tag{39}$$

and using definitions (29), (30) and (38) gives,

$$\mathscr{E}_s(\boldsymbol{u}(t)) + \mathscr{E}_f(\phi(t)) + \mathscr{R}(\phi(t)) = \mathscr{E}_s(\boldsymbol{u}(0)) + \mathscr{E}_f(\phi(0))\,, \quad \forall\, t \geq 0 \tag{40}$$

Using the initial conditions (23)–(26) gives the desired energy identity (37). □

This result provides a natural measure of stability for the exterior structural acoustics problem, and will be used to guide the design of the space–time finite element formulation described in the next section. As a specific example for the energy estimates given in (34) and (37), consider the first-order non-reflecting boundary condition defined in (15). In this case the rate of energy absorbed through the artificial boundary Γ_∞ is given by the surface integral (33) with the normal derivative replaced with

$$-\mathbb{S}_1\phi = -\frac{1}{R}\phi - \frac{1}{c}\dot{\phi} \tag{41}$$

Defining the following weighted L_2 norms on Γ_z as

$$\|\phi\|^2_{\Gamma_z} := \int_{\Gamma_z} \rho_0(\phi)^2 \, d\Gamma \tag{42}$$

$$\|\dot{\phi}\|^2_{\mathcal{Y}_z} := \int_0^t \|\dot{\phi}\|^2_{\Gamma_z} \, d\tau \tag{43}$$

then with the linear operator $\mathbb{S}_1$ defined in (15), the rate of energy transport through the artificial boundary specializes to

$$\begin{aligned} \mathscr{D}(\phi) &= \frac{1}{R}\int_{\Gamma_z} \rho_0 \dot{\phi}\phi \, d\Gamma + \frac{1}{c}\int_{\Gamma_z} \rho_0(\dot{\phi})^2 \, d\Gamma \\ &= \frac{1}{2} c_0 \frac{d}{dt}\|\phi\|^2_{\Gamma_z} + c_1\|\dot{\phi}\|^2_{\Gamma_z} \end{aligned} \tag{44}$$

where $c_0 = 1/R$ and $c_1 = 1/c$ are positive constants. An energy identity of the form (37) is obtained by integrating (44) over time with the result,

$$\mathscr{E}_s(u) + \mathscr{E}_f(\phi) + \frac{1}{2} c_0\|\phi\|^2_{\Gamma_z} + c_1\|\dot{\phi}\|^2_{\mathcal{Y}_z} = \mathscr{E}_s(u_0) + \mathscr{E}_f(\phi_0) \tag{45}$$

In the above, we have used the fact that $\phi_0 = \dot{\phi}_0 = 0$ on Γ_z. This is the stability (energy) estimate for the continuum problem with $\mathbb{S}_1$. It states that the total energy for the structure $\mathscr{E}_s$ and the fluid $\mathscr{E}_f$ plus the radiation energy absorbed through the artificial boundary Γ_z is equal to the initial energy in the system. An analogous result will be derived for the proposed space–time finite element formulation incorporating $\mathbb{S}_1$, see Theorem 7.1. Eq. (45) can also be used to prove uniqueness of the coupled structural acoustic problems with χ variables and radiation boundaries (see [27]).

4. Discontinuous Galerkin formulation

The development of the space–time finite element method follows the procedure outlined in [6], by considering an ordered partition of the open time interval, $I =]0, T[$, of the form: $0 = t_0 < t_1 < \cdots < t_N = T$, with variable time step $\Delta t_n = t_{n+1} - t_n$. Then, the time interval of interest can be written as $I = \{\cup_{n=0}^{N-1} I_n\} \cup \{t_1, t_2, \ldots, t_{N-1}\}$, where the nth open time interval is defined by

$$I_n :=]t_n, t_{n+1}[\tag{46}$$

Using this notation nth space–time slabs for the structure and fluid are defined respectively as

$$Q^s_n = \Omega_s \times I_n, \qquad Q^f_n = \Omega_f \times I_n \tag{47}$$

with boundaries $Y^s_n = \partial\Omega_s \times I_n$ and $Y^f_n = \partial\Omega_f \times I_n$. For the nth space–time slab $(n_{el})^s_n$ and $(n_{el})^f_n$ denote the number of space–time finite elements in the subdomains Q^s_n and Q^f_n, respectively. With these definitions, $Q^{s^e}_n \subset Q^s_n$ denotes the interior of the eth element in the structural domain with boundary $Y^{s^e}_n$. Similarly, $Q^{f^e}_n \subset Q^f_n$ denotes the interior of the eth element in the fluid domain, with boundary $Y^{f^e}_n$.

Fig. 2 shows an illustration of two consecutive space–time slabs Q_{n-1} and Q_n for the fluid where the superscript is omitted for clarity. Within each space–time element, the trial solution and weighting function are approximated by pth order polynomials in x and t. These functions are assumed $C^0(Q_n)$ continuous throughout each space–time slab, but are allowed to be discontinuous across the interfaces of the slabs. Assuming the function $w(x, t)$ to be discontinuous at time t_n, suppressing the argument x, the temporal jump operator is defined by

$$[\![w(t_n)]\!] := w(t_n^+) - w(t_n^-) \tag{48}$$

where

$$w(t_n^\pm) = \lim_{\epsilon \to 0\pm} w(t_n + \epsilon)$$

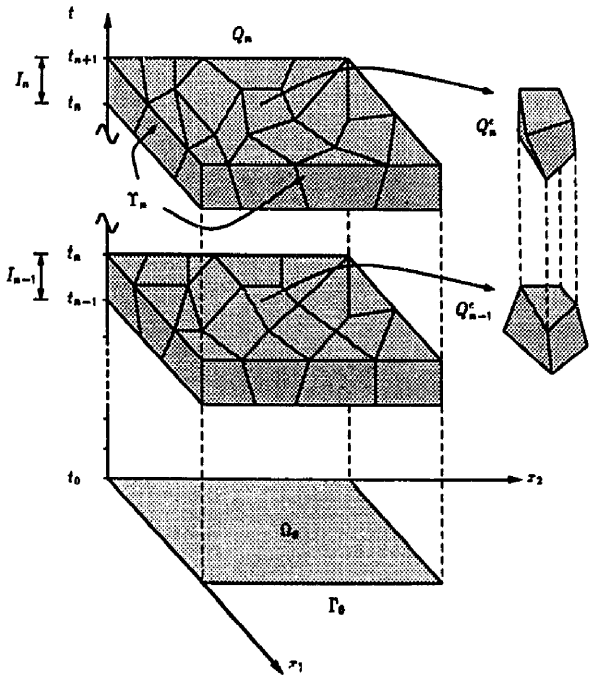

Fig. 2. Illustration of two consecutive space–time slabs with unstructured finite element meshes within a slab.

This discontinuity of the finite element functions across space–time slab interfaces, allows for the general use of high-order elements and spectral-type interpolations in both space and time, and provides freedom of changing the discretization from one time step to another. The discontinuity is also essential for the unconditional stability of the space–time method proposed in this paper. For simplicity, the collections of finite element shape functions are stated for equal-order interpolation in space–time; however it should be noted that unequal orders are allowed.

Trial structural displacements

$$\mathscr{S}^h = \bigcup_{n=0}^{N-1} \mathscr{S}_n^h, \qquad \mathscr{S}_n^h = \{\boldsymbol{u}^h(\boldsymbol{x},t) | \boldsymbol{u}^h \in (C^0(Q_n^s))^d, \boldsymbol{u}^h|_{Q_n^{se}} \in (\mathscr{P}^k(Q_n^{se}))^d\}$$

Trial fluid potential

$$\mathscr{T}^h = \bigcup_{n=0}^{N-1} \mathscr{T}_n^h, \qquad \mathscr{T}_n^h = \{\phi^h(\boldsymbol{x},t) | \phi^h \in C^0(Q_n^f), \phi^h|_{Q_n^{fe}} \in \mathscr{P}^p(Q_n^{fe})\}$$

In the above, $\mathscr{P}^k$ and $\mathscr{P}^p$ denote the space of kth order and pth order interpolation polynomials within a space–time element for the structure and fluid, respectively. Inclusion of essential boundary conditions is straightforward with the usual restrictions placed on the trial and weighting function spaces.

Before stating the space–time variational equations, it is useful to introduce the following notation.

$$\tilde{Q}_n = \bigcup_{e=1}^{(n_{el})_n} Q_n^e \quad \text{(element interiors)} \tag{49}$$

$$\tilde{Y}_n = \bigcup_{e=1}^{(n_{el})_n} Y_n^e - Y_n \quad \text{(interior mesh boundaries)} \tag{50}$$

Space–time element boundaries which coincide with the artificial boundary $(Y_\infty)_n := \Gamma_\infty \times I_n$ are denoted $(\bar{Y}_\infty)_n^e = Y_n^e \cap (Y_\infty)_n$, where the overbar indicates the closure. Using this notation, the interiors of the element boundaries restricted to the artificial boundary are defined as

$$(\tilde{Y}_\infty)_n = \bigcup_{e=1}^{(n_{el})_n} (\tilde{Y}_\infty)_n^e \tag{51}$$

The strain-energy inner product for the structure is denoted by

$$a(\boldsymbol{w}, \boldsymbol{u})_{\Omega_s} = \int_{\Omega_s} \nabla \boldsymbol{w} \cdot \boldsymbol{\sigma}(\nabla \boldsymbol{u})\, d\Omega \tag{52}$$

Standard L_2 inner products are defined as

$$(\boldsymbol{w}, \boldsymbol{u})_\Omega = \int_\Omega \boldsymbol{w} \cdot \boldsymbol{u}\, d\Omega \tag{53}$$

and equipped with norm $\|\boldsymbol{w}\|_\Omega = (\boldsymbol{w}, \boldsymbol{w})^{1/2}$. Inner products for the fluid are weighted by the fluid reference density ρ_0. Integration over element interiors is defined as

$$(w^h, \phi^h)_{\tilde{Q}_n} = \sum_{e=1}^{(n_{el})_n} \int_{Q_n^e} w^h \phi^h\, dQ \tag{54}$$

4.1. Variational equations

The space–time variational formulation for the coupled structural acoustics problem is obtained from a weighted residual of the governing equations (16)–(22) within a space–time slab and incorporates time-discontinuous jump terms across slab interfaces. The specific form of this variational equation is designed such that a priori stability and energy estimates analogous to those described in Theorem 3.1 for the continuum problem are obtained for the discrete problem.

Within each space–time slab, $n = 0, 1, \ldots, N-1$, the objective is to find $\boldsymbol{\chi}^h := \{\boldsymbol{u}^h, \boldsymbol{\phi}^h\} \in \mathcal{S}_n^h \times \mathcal{T}_n^h$, such that $\forall\, \boldsymbol{\psi}^h := \{\boldsymbol{w}^h, w^h\} \in \mathcal{V}_n^h \times \mathcal{W}_n^h$, the following coupled variational equations are satisfied,

$$B_s(\boldsymbol{w}^h, \boldsymbol{\chi}^h)_n = L_s(\boldsymbol{w}^h)_n \tag{55}$$

$$B_f(w^h, \boldsymbol{\chi}^h)_n = L_f(w^h)_n \tag{56}$$

with the following definitions,

$$B_s(\boldsymbol{w}^h, \boldsymbol{\chi}^h)_n := E_s(\boldsymbol{w}^h, \boldsymbol{u}^h)_n - A(\boldsymbol{w}^h, \boldsymbol{\phi}^h)_n \tag{57}$$

$$B_f(w^h, \boldsymbol{\chi}^h)_n := E_f(w^h, \boldsymbol{\phi}^h)_n + A(\boldsymbol{u}^h, w^h)_n + E_r(w^h, \boldsymbol{\phi}^h)_n \tag{58}$$

and

$$E_s(\boldsymbol{w}^h, \boldsymbol{u}^h)_n := (\dot{\boldsymbol{w}}^h, \rho_s \ddot{\boldsymbol{u}}^h)_{Q_n^s} + a(\dot{\boldsymbol{w}}^h, \boldsymbol{u}^h)_{Q_n^s} + (\boldsymbol{w}^h(t_n^+), \rho_s \dot{\boldsymbol{u}}^h(t_n^-))_{\Omega_s} + a(\boldsymbol{w}^h(t_n^+), \boldsymbol{u}^h(t_n^+))_{\Omega_s} \tag{59}$$

$$E_f(w^h, \boldsymbol{\phi}^h)_n := (\dot{w}^h, a^2 \ddot{\boldsymbol{\phi}}^h)_{Q_n^f} + (\nabla \dot{w}^h, \nabla \boldsymbol{\phi}^h)_{Q_n^f} + (\dot{w}^h(t_n^+), a^2 \dot{\boldsymbol{\phi}}^h(t_n^+))_{\Omega_f} + (\nabla w^h(t_n^+), \nabla \boldsymbol{\phi}^h(t_n^+))_{\Omega_f} \tag{60}$$

$$A(\boldsymbol{w}^h, \boldsymbol{\phi}^h)_n := (\dot{\boldsymbol{w}}^h, \rho_0 \dot{\boldsymbol{\phi}}^h \boldsymbol{n})_{(Y_I)_n} \tag{61}$$

$$L_s(\boldsymbol{w}^h)_n := (\dot{\boldsymbol{w}}^h, \bar{\boldsymbol{t}})_{(Y_\sigma)_n} + (\dot{\boldsymbol{w}}^h(t_n^+), \rho_s \dot{\boldsymbol{u}}^h(t_n^-))_{\Omega_s} + a(\boldsymbol{w}^h(t_n^+), \boldsymbol{u}^h(t_n^-))_{\Omega_s} \tag{62}$$

$$L_f(w^h)_n := (\dot{w}^h, f)_{Q_n^f} + (\dot{w}^h(t_n^+), a^2 \dot{\boldsymbol{\phi}}^h(t_n^-))_{\Omega_f} + (\nabla w^h(t_n^+), \nabla \boldsymbol{\phi}^h(t_n^-))_{\Omega_f} \tag{63}$$

The operator $E_r(w^h, \boldsymbol{\phi}^h)_n$, incorporates the time-dependent non-reflecting boundary operators $\mathbb{S}_m$ as natural boundary conditions, i.e. they are enforced weakly through integration over both the artificial

boundary Γ_∞ and the time interval I_n. The formal definition of this boundary operator with details for the implementation of the non-reflecting boundary conditions are given in the next section.

In order to guarantee a stable space–time finite element algorithm, the coupled variational equations (55) and (56) are constructed in a form which is consistent with the energy (stability) estimates given in Lemma 3.1 and Theorem 3.1 for the continuum problem. The design criteria then is to construct a coupled variational equation such that the natural energy norm emanating from this variational equation satisfies a stability (energy) identity analogous to that obtained for the continuum problem. A key feature is the use of the time derivative (time rate of change) of ψ^h, i.e. $\dot{\psi}^h := \{\dot{w}^h, \dot{w}^h\}$, as the weighting function in the terms evaluated over Q_n in (59) and (60). With this choice of weighting function, the form of these terms are consistent with the time rate of change of structural acoustic energy defined in (34)–(36). In the operator $E_s(\cdot,\cdot)_n$, the terms evaluated over Q_n^s, act to weakly enforce the momentum balance in the structure and are identical to Eq. (105) in [6]. In $E_f(\cdot,\cdot)_n$, the terms evaluated over Q_n^f, act to weakly enforce the scalar wave equation in the fluid within the interior of the nth space–time slab.

The terms evaluated over the structural domain Ω_s in (59) and (62), together with the terms evaluated over the fluid domain Ω_f in (60) and (63) act to weakly enforce continuity across space–time interfaces. Weak enforcement of the velocity $v^h = \nabla\phi^h$ and pressure $p^h = -\rho_0\dot{\phi}^h$ for the acoustic fluid is prescribed through the temporal jump operators associated with (60) and (63), i.e.

$$(\dot{w}^h(t_n^+), a^2\ [\![\dot{\phi}^h(t_n)]\!]\ )_{\Omega_f} + (\nabla w^h(t_n^+), \underbrace{[\![\nabla\phi^h(t_n)]\!]}_{\text{velocity jump}})_{\Omega_f}$$

pressure jump

Similar temporal jump operators associated with (59) and (62) defined over Ω_s act to weakly enforce structural velocities and stresses across time steps. The specific form of these jump operators are designed such that continuity is weakly enforced via a kinetic and strain energy inner product for the structure and similarly a kinetic and potential energy inner product for the acoustic fluid. These jump conditions are the mechanism by which information is advanced from one space–time slab to the next. Physically, they add a consistent numerical dissipation into the algorithm which helps control any oscillations that may occur in the vicinity of discontinuities or sharp gradients in the solution [7].

Fluid–structure interaction is accomplished through the coupling operators $A(\cdot,\cdot)_n$ integrated over the fluid–structure interface $(Y_i)_n = \Gamma_i \times I_n$. These coupling terms appearing in (57) and (58) weakly enforce the acoustic pressure interface condition (11) and continuity of normal velocity condition (12), respectively. The fact that the coupling operators in both (57) and (58) are of the same form; namely (61), follows directly from the choice of $\chi^h := \{u^h, \phi^h\}$ for the structure–fluid solution variables and the consistent weighting $\dot{\psi}^h := \{\dot{w}^h, \dot{w}^h\}$. This global symmetry property of the coupled space–time variational equations facilitates the establishment of stability and convergence proofs for the coupled finite element formulation in a manner similar to that obtained for the continuum problem.

REMARK 1. The method is applied in one space–time slab at a time; data from the end of the previous slab are employed as initial conditions for the current slab. Because the solution is weakly enforced across slab interfaces, the finite element mesh may change from one slab to the next and it is not required that the meshes match across the discrete time levels. This is especially useful for adaptive schemes where the finite element discretization can be refined/unrefined within space–time slabs to track wave fronts as they propagate along space–time characteristics.

REMARK 2. In [6] an extension of the time-discontinuous Galerkin space–time formulation is given where independent interpolation functions are used for the solution and its time derivative, e.g. for elastodynamics, independent interpolations are used for the displacements and velocities. In [27, 28] an extension of the formulation presented in this paper is developed as a multi-field formulation incorporating second-order non-reflecting boundary conditions with independent velocity potential and pressure variables for the fluid. This multi-field formulation allows for a variety of combinations of high-order interpolations, including equal-order for ϕ^h and p^h.

4.2. Non-reflecting boundary conditions

The linear mapping $\mathbb{S}_m\phi$ defined previously in (13) is assumed to take the following abstract form,

$$\mathbb{S}_m\phi = \sum_{j=0}^{m} C_j\left[\frac{\partial^j\phi}{\partial t^j}\right] \quad \text{on } Y_x := \Gamma_x \times I_n \tag{64}$$

In this expression, the index m reflects the order of the temporal derivatives appearing in the operator, and C_j, $j = 0, 1, \ldots, m$, are spatial operators that may be local differential operators that couple only adjacent points on the artificial boundary, or non-local integral operators that couple all points on the artificial boundary Γ_x. Specific examples of time-dependent non-reflecting boundary conditions which can be expressed in this general form are discussed in detail in [25]. Here, we note that the first-order operator ($m = 1$) defined previously in (15) conform to this representation with the spatial operators C_j, $j = 0, 1$ reducing to $1/R$ and $1/c$.

In general, boundary conditions of the form (64) provide increasing accuracy with the order m; however, as the order increases, they become increasingly difficult to implement in a standard semidiscrete finite element setting due to the occurrence of high-order time derivatives on the truncation boundary Y_x. Semidiscrete methods for second-order hyperbolic wave equations, which discretize the spatial domain with finite elements, lead to a second-order system of ordinary differential equations in time. These ordinary differential equations are then integrated using standard finite difference algorithms such as the Newmark family of time integrators. Since standard semidiscrete algorithms are restricted to integrating up to second-order time derivatives, their application to (64) are limited to orders $m \leq 2$ only.

Space–time finite element methods, in which the solution is allowed to be discontinuous across space–time slabs places no restriction on the order m of time derivative appearing in the operator $\mathbb{S}_m$. Since continuity is enforced weakly between time steps, standard C^0 continuous interpolation functions in the time coordinate can be used up to the order dictated by the operator $\mathbb{S}_m$. An advantage of the space–time formulation is that the order of the temporal interpolation can be increased near the non-reflecting boundary so that temporal accuracy is increased locally to a level required by the boundary condition. It is this special property of the discontinuous Galerkin formulation that provides for the potential to directly implement (64) up to any order desired. It is noted however, that high-order non-reflecting boundary conditions beyond second-order may involve high-order spatial derivatives appearing in C_j, that require increased continuity in the spatial coordinate. In this case special local boundary elements which incorporate high-order continuous spatial basis functions would be needed (see e.g. [29]). In the discussion to follow, we describe how the time-discontinuous Galerkin space–time method provides a natural variational setting for the incorporation of non-reflecting boundary conditions of the form (64), and how under certain conditions on the boundary operators stability and convergence can be proved a priori.

For boundary operators up to second-order $m = 1, 2$, the bilinear form $E_r(\cdot,\cdot)_n$ appearing in the space–time variational equation (58), is defined as:

For $m = 1$,

$$E_r(w^h, \phi^h)_n := (\dot{w}^h, \mathbb{S}_1\phi^h)_{(Y_x)_n} + d_0(w^h(t_n^+), [\![\phi^h(t_n)]\!])_{\Gamma_x} \tag{65}$$

For $m = 2$,

$$E_r(w^h, \phi^h)_n := (\dot{w}^h, \mathbb{S}_2\phi^h)_{(Y_x)_n} + d_2(\dot{w}^h(t_n^+), [\![\dot{\phi}^h(t_n)]\!])_{\Gamma_x} + d_0(w^h(t_n^+), [\![\phi^h(t_n)]\!])_{\Gamma_x} \tag{66}$$

The term evaluated over $(Y_x)_n := \Gamma_x \times I_n$ acts to weakly enforce the non-reflecting boundary condition (64) over the time interval $]t_n, t_{n+1}[$ and Γ_x. The form of this boundary operator is guided by the definition of the acoustic intensity given in (33). Replacing the trial solution with w^h, we have

$$(\dot{w}^h, \mathbb{S}_m w^h)_{(Y_x)_n} = \int_{t_n}^{t_{n+1}} \mathscr{Q}(w^h)\,\mathrm{d}t \tag{67}$$

indicating that this term represents an acoustic radiation inner product integrated over the time interval I_n. As a specific example, consider the first-order, ($m = 1$), non-reflecting boundary condition defined previously in (15) and repeated here as

$$\mathbb{S}_1\phi = C_0\phi + C_1\dot{\phi} \tag{68}$$

where the spatial operators reduce to the positive values $C_1 = 1/R$ and $C_2 = 1/c$. For this case, the acoustic radiation operator takes the form

$$(\dot{w}^h, \mathbb{S}_1\phi^h)_{(Y_x)_n} := d_0(\dot{w}^h, \phi^h)_{(Y_x)_n} + d_1(\dot{w}^h, \dot{\phi}^h)_{(Y_x)_n} \tag{69}$$

where the index on the bilinear operators d_0 and d_1 reflects the order of the time derivative appearing on the trial solution. For this simple case, the bilinear operators reduce to

$$d_0(\dot{w}^h, \phi^h)_{(Y_x)_n} = \frac{1}{R}\int_{I_n}^{t_{n+1}}\int_{\Gamma_x} \rho_0 \dot{w}^h \phi^h \, d\Gamma \, dt \tag{70}$$

$$d_1(\dot{w}^h, \dot{\phi}^h)_{(Y_x)_n} = \frac{1}{c}\int_{I_n}^{t_{n+1}}\int_{\Gamma_x} \rho_0 \dot{w}^h \dot{\phi}^h \, d\Gamma \, dt \tag{71}$$

Similarly, extending the sequence (64) to second-order ($m = 2$),

$$\mathbb{S}_2\phi = C_0\phi + C_1\dot{\phi} + C_2\ddot{\phi} \tag{72}$$

the radiation operator reduces to

$$(\dot{w}^h, \mathbb{S}_2\phi^h)_{(Y_x)_n} := d_0(\dot{w}^h, \phi^h)_{(Y_x)_n} + d_1(\dot{w}^h, \dot{\phi}^h)_{(Y_x)_n} + d_2(\dot{w}^h, \ddot{\phi}^h)_{(Y_x)_n} \tag{73}$$

The form of the bilinear operators d_j depends on the local or non-local character of the spatial operators C_j appearing in (72). The index for the operators d_j, $j = 0, 1, 2$, reflects the order of the time derivative on the trial solution appearing in the operator. Specific examples for $\mathbb{S}_2$ are given in [25].

The terms evaluated over the space–time slab interface at the boundary Γ_x in (65) and (66) act to weakly enforce continuity of the trial solution across space–time slab interfaces. The specific form of these operators are designed such that continuity of the artificial boundary Γ_x is weakly enforced in a form which is consistent with the radiation boundary term evaluated over $(Y_x)_n$. Thus, for $m = 2$, the form of the consistent temporal jump operators $[\![\phi^h(t_n)]\!]$ and $[\![\dot{\phi}^h(t_n)]\!]$ embedded in the last two terms of (66) depend on the form of the spatial derivatives appearing in the bilinear operators $d_0(\cdot,\cdot)_{(Y_x)_n}$ and $d_2(\cdot,\cdot)_{(Y_x)_n}$ given in (73). These consistent temporal jump operators are required in order to ensure that the discontinuous Galerkin solution is unconditionally stable and are the crucial element that enable generalization of the space–time finite element method to handle exterior domains. Note that no jump operator is needed for the term corresponding to $d_1(\dot{w}^h, \dot{\phi}^h)_{(Y_x)_n}$ in (73). The reason for this becomes clear from the stability analysis described in the next section where it is shown that this term naturally leads to a well-defined norm, requiring no additional stabilization.

For $m = 1$, since the first-order non-reflecting boundary condition defined in (15) involves only first-order temporal derivatives, the only consistent jump operator needed is $d_0(\cdot,\cdot)_{\Gamma_x}$. The form of this jump operator follows from (70), i.e.

$$d_0(w^h(t_n^+), [\![\phi^h(t_n)]\!])_{\Gamma_x} = \frac{1}{R}\int_{\Gamma_x} \rho_0 w^h(t_n^+), [\![\phi^h(t_n)]\!] \, d\Gamma \tag{74}$$

To facilitate the stability and convergence proofs incorporating non-reflecting boundary conditions, boundary operators are assumed to be spatially non-negative, i.e.

$$d_j(w^h, w^h)_{\Gamma_x} \geq 0, \quad j = 0, 1, 2 \quad \forall\, w^h \in \mathcal{W}^h \tag{75}$$

Examining the boundary operators defined in (70) and (71) for $\mathbb{S}_1$, it is clear that these operators satisfy condition (75) explicitly, i.e.

$$d_0(w^h, w^h)_{\Gamma_2} = C_0 \|w^h\|^2_{\Gamma_2} \geq 0 \tag{76}$$

$$d_1(w^h, w^h)_{\Gamma_2} = C_1 \|w^h\|^2_{\Gamma_2} \geq 0 \tag{77}$$

where $C_0 = 1/R$ and $C_1 = 1/c$ are positive constants, and $\|w^h\|^2_{\Gamma_2}$ is the weighted L_2 norm restricted to the boundary Γ_2.

5. Galerkin least-squares stabilization

In order to enhance the stability of the basic time-discontinuous Galerkin space–time formulation, and to prove that the method converges for arbitrary space–time discretizations, local residuals of the governing differential equations in the form of least-squares operators are added to the variational equations (55) and (56). Stabilized methods of this type are referred to as Galerkin Least-Squares (GLS) methods [8]. The time-discontinuous GLS formulation for coupled structural acoustics is stated formally as:

Within each space–time slab, $n = 0, 1, \ldots, N-1$: Find $\boldsymbol{\chi}^h := \{\boldsymbol{u}^h, \phi^h\} \in \mathcal{S}^h_n \times \mathcal{T}^h_n$, such that $\forall \boldsymbol{\psi}^h := \{\boldsymbol{w}^h, w^h\} \in \mathcal{V}^h_n \times \mathcal{W}^h_n$,

$$B^{\mathrm{s}}_{\mathrm{GLS}}(\boldsymbol{w}^h, \boldsymbol{\chi}^h)_n = L^{\mathrm{s}}_{\mathrm{GLS}}(\boldsymbol{w}^h)_n \tag{78}$$

$$B^{\mathrm{f}}_{\mathrm{GLS}}(w^h, \boldsymbol{\chi}^h)_n = L^{\mathrm{f}}_{\mathrm{GLS}}(w^h)_n \tag{79}$$

where

$$B^{\mathrm{s}}_{\mathrm{GLS}}(\boldsymbol{w}^h, \boldsymbol{\chi}^h)_n = B_{\mathrm{s}}(\boldsymbol{w}^h, \boldsymbol{\chi}^h)_n + B^{\mathrm{s}}_{\mathrm{LS}}(\boldsymbol{w}^h, \boldsymbol{\chi}^h)_n \tag{80}$$

$$L^{\mathrm{s}}_{\mathrm{GLS}}(\boldsymbol{w}^h)_n = L_{\mathrm{s}}(\boldsymbol{w}^h)_n + L^{\mathrm{s}}_{\mathrm{LS}}(\boldsymbol{w}^h)_n \tag{81}$$

similarly,

$$B^{\mathrm{f}}_{\mathrm{GLS}}(w^h, \boldsymbol{\chi}^h)_n = B_{\mathrm{f}}(w^h, \boldsymbol{\chi}^h)_n + B^{\mathrm{f}}_{\mathrm{LS}}(w^h, \boldsymbol{\chi}^h)_n \tag{82}$$

$$L^{\mathrm{f}}_{\mathrm{GLS}}(w^h)_n = L_{\mathrm{f}}(w^h)_n + L^{\mathrm{f}}_{\mathrm{LS}}(w^h)_n \tag{83}$$

The least-squares addition to the Galerkin variational equation for the structure is an extension of Eqs. (101) and (102) in [6] and is defined as:

$$\begin{aligned} B^{\mathrm{s}}_{\mathrm{LS}}(\boldsymbol{w}^h, \boldsymbol{\chi}^h)_n := {} & (\mathcal{L}_{\mathrm{s}}\boldsymbol{w}^h, \rho_{\mathrm{s}}^{-1}\tau\mathcal{L}_{\mathrm{s}}\boldsymbol{u}^h)_{\tilde{Q}^{\mathrm{s}}_n} + (\llbracket\boldsymbol{\sigma}(\nabla\boldsymbol{w}^h)(\boldsymbol{x})\rrbracket\cdot\boldsymbol{n}, \rho_{\mathrm{s}}^{-1}s\llbracket\boldsymbol{\sigma}(\nabla\boldsymbol{u}^h)(\boldsymbol{x})\rrbracket\cdot\boldsymbol{n})_{\tilde{Y}^{\mathrm{s}}_n} \\ & + (\boldsymbol{\sigma}(\nabla\boldsymbol{w}^h)\cdot\boldsymbol{n}, \rho_{\mathrm{s}}^{-1}s\boldsymbol{\sigma}(\nabla\boldsymbol{u}^h)\cdot\boldsymbol{n})_{(Y_{\mathrm{s}})_n} + (\mathcal{L}_1\boldsymbol{\psi}^h, \rho_{\mathrm{s}}^{-1}s\mathcal{L}_1\boldsymbol{\chi}^h)_{(Y_{\mathrm{f}})_n} \end{aligned} \tag{84}$$

$$L^{\mathrm{s}}_{\mathrm{LS}}(\boldsymbol{w}^h)_n := (\boldsymbol{\sigma}(\nabla\boldsymbol{w}^h)\cdot\boldsymbol{n}, \rho_{\mathrm{s}}^{-1}s\bar{\boldsymbol{t}})_{(Y_{\sigma})_n} \tag{85}$$

where the residual for the structure is given by the equations of motion $\mathcal{L}_{\mathrm{s}}\boldsymbol{u}^h := \rho_{\mathrm{s}}\ddot{\boldsymbol{u}}^h - \nabla\cdot\boldsymbol{\sigma}(\nabla\boldsymbol{u}^h)$ and $\mathcal{L}_1\boldsymbol{\chi}^h := \boldsymbol{\sigma}(\nabla\boldsymbol{u}^h)\cdot\boldsymbol{n} - \rho_0\dot{\phi}^h\boldsymbol{n}$ is the residual for the traction interface boundary condition.

Similarly for the fluid domain, the least-square addition takes the form,

$$\begin{aligned} B^{\mathrm{f}}_{\mathrm{LS}}(w^h, \boldsymbol{\chi}^h)_n := {} & (\mathcal{L}_{\mathrm{f}}w^h, c^2\tau\mathcal{L}_{\mathrm{f}}\phi^h)_{\tilde{Q}^{\mathrm{f}}_n} + (\mathcal{L}_r w^h, c^2 s\mathcal{L}_r\phi^h)_{(\tilde{Y}_{\mathrm{f}})_n} \\ & + (\llbracket w^h_{,n}(\boldsymbol{x})\rrbracket, c^2 s\llbracket\phi^h_{,n}(\boldsymbol{x})\rrbracket)_{\tilde{Y}^{\mathrm{f}}_n} + (\mathcal{L}_2\boldsymbol{\psi}^h, c^2 s\mathcal{L}_2\boldsymbol{\chi}^h)_{(Y_{\mathrm{f}})_n} \end{aligned} \tag{86}$$

$$L^{\mathrm{f}}_{\mathrm{LS}}(w^h)_n := (\mathcal{L}_{\mathrm{f}}w^h, c^2\tau f)_{\tilde{Q}^{\mathrm{f}}_n} \tag{87}$$

where the normal derivative is denoted $\phi^h_{,n} = \nabla\phi^h\cdot\boldsymbol{n}$ and

$$\mathcal{L}_{\mathrm{f}}\phi^h := a^2\ddot{\phi}^h - \nabla^2\phi^h \tag{88}$$

$$\mathscr{L}_1\phi^h := \phi^h_{,n} + \mathbb{S}_m\phi^h \tag{89}$$

$$\mathscr{L}_2\chi^h := \dot{u}^h \cdot n - \phi^h_{,n} \tag{90}$$

The GLS weighting parameter τ has dimensions of time and can be interpreted as an intrinsic time-scale, while the parameter s has dimensions of inverse speed and is a slowness scale. For the structural domain, the intrinsic time scale τ and slowness scale s are matrices of size $d \times d$. These GLS weighting parameters are functions that are dependent on element size and interpolation order, and may be designed to improve stability without degrading the accuracy of the underlying time-discontinuous Galerkin formulation. When these GLS parameters are set to zero, the formulation specializes to the discontinuous Galerkin method.

From a Fourier analysis of the time-discontinuous method for first-order hyperbolic equations, Shakib and Hughes [30] have shown that GLS parameters can be optimized to achieve higher-order accuracy and minimize undesirable high frequency response without introducing excessive algorithmic damping in the low frequency regime. Fourier analysis has also been used to design optimal GLS parameters to enhance the stability and accuracy of solutions to the related reduced wave equation (Helmholtz equation) governing time-harmonic acoustics in the frequency domain (see [9–12]).

For second-order hyperbolic systems, a practical value for τ and s as suggested by Hughes and Hulbert [6] is

$$\tau = \Delta x\, s = \frac{1}{2}\frac{\Delta x}{c}\boldsymbol{I} \tag{91}$$

where $\boldsymbol{I}$ is the $d \times d$ identity matrix, c_L is the dilitational wave speed and Δx is interpreted as a local element size in the space dimension. Similar expressions can be defined for τ and s, e.g. $\tau = \Delta x\, s = \Delta x/2c$, or $\tau = \Delta t/2$. In Hulbert [32], the intrinsic time-scale used for a uniform quadratic interpolation was taken as

$$\tau = \frac{\Delta t}{4\sqrt{1+C^4}} \tag{92}$$

where C is the Courant number. While the definitions of these parameters are crucial to GLS performance, for the purposes of proving convergence, it is sufficient that they be dimensionally consistent. Both slowness and time scale parameters are needed in the convergence proof. However, from an algorithmic point of view, the implementation of the terms involving the slowness parameters involve unconventional and expensive calculations. As indicated by Hulbert [31] and the results from our numerical experience in Section 7, optimal convergence rates are achieved with the omission of the slowness parameters, and therefore in practice, it is suggested that these parameters be set to zero, i.e. $s = 0$ and $s = \mathbf{0}$.

For numerical solutions exhibiting sharp gradients or discontinuities due to shocks, non-linear discontinuity capturing operators are available to help further control oscillations that may occur in the solution [32]. However, for linear structural acoustics problems, the added expense resulting from a non-linear solve as required from the use of these discontinuity capturing operators is not justified.

6. Euler–Lagrange equations

Weak enforcement of the governing Euler–Lagrange equations for the structure is exposed by integrating (78) by parts to yield the following weighted residual expression,

$$\begin{aligned}
0 &= B^h_{\mathrm{GLS}}(w^h, \chi^h)_n - L^h_{\mathrm{GLS}}(w^h)_n \\
&= (\dot{w}^h + \rho_s^{-1}\tau\mathscr{L}_s w^h, r_s^h)_{\bar{Q}^h_n} + (\dot{w}^h + \rho_s^{-1}s\sigma(\nabla w^h)\cdot n, \sigma(\nabla u^h)\cdot n - \bar{t})_{(\Gamma_\sigma)_n} \\
&\quad + (\dot{w}^h + \rho_s^{-1}s[\![\sigma(\nabla w^h)(x)]\!]\cdot n, [\![\sigma(\nabla u^h)(x)]\!]\cdot n)_{(\tilde{\Gamma}^h)_n} + (\dot{w}^h + \rho_s^{-1}s\mathscr{L}_1\psi, r_1^h)_{(\Omega^h)_n} \\
&\quad + (\dot{w}^h(t_n^+), [\![\dot{u}^h(t_n)]\!])_{\Omega_h} + a(w^h(t_n^+), [\![u^h(t_n)]\!])_{\Omega_h}
\end{aligned} \tag{93}$$

where

$$\begin{aligned} r_s^h &= \mathcal{L}_s u^h \quad \text{(equation of motion)} \\ r_1^h &= \mathcal{L}_1 \chi^h \quad \text{(coupling boundary condition)} \end{aligned} \tag{94}$$

The second line in (93) describes the weak enforcement of the momentum balance residual r_s^h, for the structure within a space–time slab; the third line acts to weakly enforce the prescribed traction at the boundary Γ_{s_t}; while the terms in line four define the weak enforcement of the traction continuity across element boundaries. This term arises from integration-by-parts over the spatial domain. Line five describes the weak enforcement of the traction coupling boundary condition r_1^h, at the interface between the structure and the fluid. The last two lines in (93) show how continuity between space–time slab interfaces is weakly enforced via a total structural energy inner product.

Similarly for the fluid domain, integrating (79) by parts yields,

$$\begin{aligned} 0 &= B_{\mathrm{GLS}}^{\mathrm{f}}(w^h, \chi^h)_n - L_{\mathrm{GLS}}^{\mathrm{f}}(w^h)_n \\ &= (\dot{w}^h + \tau c^2 \mathcal{L}_{\mathrm{f}} w^h, r_{\mathrm{f}}^h)_{Q_n^{\mathrm{f}}} + (\dot{w}^h + s c^2 \mathcal{L}_r w^h, r_r^h)_{(\Gamma_{s_t})_n} + (\dot{w}^h + s c^2 [\![w_{,n}^h(x)]\!], [\![\phi_{,n}^h(x)]\!])_{(\Gamma^{\mathrm{f}})_n} \\ &\quad + (\dot{w}^h + s c^2 \mathcal{L}_2 \psi, r_2^h)_{(\Gamma_{\mathrm{f}})_n} + (\dot{w}^h(t_n^+), a^2 [\![\dot{\phi}^h(t_n)]\!])_{\Omega_{\mathrm{f}}} + (\nabla w^h(t_n^+), [\![\nabla \phi^h(t_n)]\!])_{\Omega_{\mathrm{f}}} \\ &\quad + d_2(\dot{w}^h(t_n^+), [\![\dot{\phi}^h(t_n)]\!])_{\Gamma_r} + d_0(w^h(t_n^+), [\![\phi^h(t_n)]\!])_{\Gamma_r} \end{aligned} \tag{95}$$

where

$$\begin{aligned} r_{\mathrm{f}}^h &= \mathcal{L}_{\mathrm{f}} \phi^h - f \quad \text{(wave equation)} \\ r_r^h &= \mathcal{L}_r \phi^h \quad \text{(radiation boundary condition)} \\ r_2^h &= \mathcal{L}_2 \chi^h \quad \text{(coupling boundary condition)} \end{aligned} \tag{96}$$

The second line in (95) describes the weak enforcement of the wave equation r_{f}^h, over the space–time slab; the third line acts to weakly enforce the non-reflecting boundary conditions r_r^h, at the artificial boundary; while the terms in line four define the weak enforcement of the gradient continuity in space. This term arises from integration-by-parts over the space–time domain. The notation $[\![\phi_{,n}^h(x)]\!] = \phi_{,n}^h(x^+, t) - \phi_{,n}^h(x^-, t)$ is defined as the spatial jump in the gradient across element boundaries. Line five describes the weak enforcement of the kinematic coupling boundary condition r_2^h at the interface between the fluid and the structure.

The last four lines in (95) show how continuity of the solution is weakly enforced across space–time slabs through the temporal jump operators. Within the domain Ω_{f}, continuity is weakly enforced via a total acoustic energy inner product. At the artificial boundary Γ_r, continuity is weakly enforced via the radiation boundary operators $d_2(\cdot,\cdot)_{\Gamma_r}$ and $d_0(\cdot,\cdot)_{\Gamma_r}$. These additional operators are needed in order to ensure stability and are the crucial element that enable generalization of the time-discontinuous space–time finite element method to handle non-reflecting boundary conditions.

Examining the Euler–Lagrange equations, it is clear that as a result of being a residual based method, the space–time finite element formulation is consistent, in the sense that the error in the finite element solution is orthogonal with respect to

$$B_{\mathrm{GLS}}^{\mathrm{s}}(w^h, E)_n = 0 \tag{97}$$

$$B_{\mathrm{GLS}}^{\mathrm{f}}(w^h, E)_n = 0 \tag{98}$$

where $E = \chi^h - \chi$ is the error; in components $E = \{u^h - u, \phi^h - \phi\}$. Clearly, the time-discontinuous Galerkin formulation with $(\tau = 0, s = 0)$ and/or $(\tau = 0, s = 0)$ also satisfies a consistency condition.

7. Stability and convergence analysis

In this section we prove that the space–time variational formulation inherits a stability estimate of the form given by Theorem 3.1 for the continuum problem. Using this estimate we conclude that the proposed space–time method for the coupled structural acoustics problem with the direct implementa-

tion of radiation boundary conditions is unconditionally stable and converges at an optimal rate. The algorithm is termed unconditionally stable if, in the absence of forcing terms and for arbitrary initial conditions, the computed total energy for the system plus the radiation energy absorbed through the artificial boundary is always less than or equal to the initial energy in the system for arbitrary step-sizes.

In the following analysis a series of Lemmas are proved which give the strong coercivity (positive-definite) conditions for the coupled variational equations. Using these results, we then establish an energy decay inequality (stability condition) for the coupled space–time algorithm which is the discrete counterpart to the energy estimate obtained for the continuum problem. As a prelude to the more complicated fluid–structure interaction problem, a priori error estimates are obtained for the uncoupled acoustics problem with non-reflecting boundary conditions. We then return to the coupled problem, where error estimates are given for the coupled fluid–structure system.

7.1. Preliminaries

Summing (79) over the time slabs and after rearranging terms we have

$$B^{\mathrm{f}}_{\mathrm{GLS}}(w^h, \chi^h) = E_{\mathrm{f}}(w^h, \phi^h) + A(u^h, w^h) + E_{\mathrm{r}}(w^h, \phi^h) + \sum_{n=0}^{N-1} B^{\mathrm{f}}_{\mathrm{LS}}(w^h, \chi^h)_n \tag{99}$$

$$L^{\mathrm{f}}_{\mathrm{GLS}}(w^h) = \sum_{n=0}^{N-1} \{(\dot{w}^h, f)_{Q^{\mathrm{f}}_n} + L^{\mathrm{f}}_{\mathrm{LS}}(w^h)_n\} + (\dot{w}^h(0^+), a^2\dot{\phi}_0)_{\Omega_{\mathrm{f}}} + (\nabla w^h(0^+), \nabla\phi_0)_{\Omega_{\mathrm{f}}} \tag{100}$$

where the global operators are defined as

$$E_{\mathrm{f}}(w^h, \phi^h) := E_2(w^h, \phi^h) + E_0(w^h, \phi^h) \tag{101}$$

$$E_{\mathrm{r}}(w^h, \phi^h) := D_2(w^h, \phi^h) + D_1(w^h, \phi^h) + D_0(w^h, \phi^h) \tag{102}$$

$$A(u^h, w^h) := \sum_{n=0}^{N-1} (\dot{u}^h, \rho_0 \dot{w}^h \boldsymbol{n})_{(\Gamma_{\mathrm{f}})_n} \tag{103}$$

and

$$E_2(w^h, \phi^h) = \sum_{n=0}^{N-1} (\dot{w}^h, a^2\ddot{\phi}^h)_{Q^{\mathrm{f}}_n} + \sum_{n=1}^{N-1} (\dot{w}^h(t_n^+), a^2[\![\dot{\phi}^h(t_n)]\!])_{\Omega_{\mathrm{f}}} + (\dot{w}^h(0^+), a^2\dot{\phi}^h(0^+))_{\Omega_{\mathrm{f}}} \tag{104}$$

$$E_0(w^h, \phi^h) = \sum_{n=0}^{N-1} (\nabla\dot{w}^h, \nabla\phi^h)_{Q^{\mathrm{f}}_n} + \sum_{n=0}^{N-1} (\nabla w^h(t_n^+), [\![\nabla\phi^h(t_n)]\!])_{\Omega_{\mathrm{f}}} + (\nabla w^h(0^+), \nabla\phi^h(0^+))_{\Omega_{\mathrm{f}}} \tag{105}$$

$$D_2(w^h, \phi^h) = \sum_{n=0}^{N-1} d_2(\dot{w}^h, \ddot{\phi}^h)_{(\Gamma_{\mathrm{s}})_n} + \sum_{n=0}^{N-1} d_2(\dot{w}^h(t_n^+), [\![\dot{\phi}^h(t_n)]\!])_{\Gamma_{\mathrm{s}}} + d_2(\dot{w}^h(0^+), \dot{\phi}^h(0^+))_{\Gamma_{\mathrm{s}}} \tag{106}$$

$$D_0(w^h, \phi^h) = \sum_{n=0}^{N-1} d_0(\dot{w}^h, \phi^h)_{(\Gamma_{\mathrm{s}})_n} + \sum_{n=0}^{N-1} d_0(w^h(t_n^+), [\![\phi^h(t_n)]\!])_{\Gamma_{\mathrm{s}}} + d_0(w^h(0^+), \phi^h(0^+))_{\Gamma_{\mathrm{s}}} \tag{107}$$

$$D_1(w^h, \phi^h) = \sum_{n=0}^{N-1} d_1(\dot{w}^h, \dot{\phi}^h)_{(\Gamma_{\mathrm{s}})_n} \tag{108}$$

such that

$$B^{\mathrm{f}}_{\mathrm{GLS}}(w^h, \chi^h) = L^{\mathrm{f}}_{\mathrm{GLS}}(w^h) \tag{109}$$

Similarly for the structure, summing (78) over the time slabs, we obtain:

$$B^{\mathrm{s}}_{\mathrm{GLS}}(w^h, \chi^h) = L^{\mathrm{s}}_{\mathrm{GLS}}(w^h) \tag{110}$$

where

$$B^{\flat}_{\mathrm{GLS}}(w^h, \chi^h) = E_{\flat}(w^h, u^h) - A(w^h, \phi^h) + \sum_{n=0}^{N-1} B^{\flat}_{\mathrm{LS}}(w^h, \chi^h)_n \tag{111}$$

$$L^{\flat}_{\mathrm{GLS}}(w^h) = \sum_{n=0}^{N-1} \{(\dot{w}^h, \bar{t})_{(\Gamma_h)_n} + L^{\flat}_{\mathrm{LS}}(w^h)_n\} + (\dot{w}^h(0^+), \rho_{\flat} u_0)_{\Omega_{\flat}} + a(w^h(0^+), u_0)_{\Omega_{\flat}} \tag{112}$$

and

$$E_{\flat}(w^h, u^h) = \sum_{n=0}^{N-1} (\dot{w}^h, \rho_{\flat} \ddot{u}^h)_{Q^{\flat}_n} + \sum_{n=0}^{N-1} (\dot{w}^h(t_n^+), \rho_{\flat}[\![\dot{u}^h(t_n)]\!])_{\Omega_{\flat}} + (\dot{w}^h(0^+), \rho_{\mathrm{s}} \dot{u}^h(0^+))_{\Omega_{\flat}}$$
$$+ \sum_{n=0}^{N-1} a(\dot{w}^h, u^h)_{Q^{\flat}_n} + \sum_{n=0}^{N-1} a(w^h(t_n^+), [\![u^h(t_n)]\!])_{\Omega_{\flat}} + a(w^h(0^+), u^h(0^+))_{\Omega_{\flat}} \tag{113}$$

From (97) and (98) it follows that for a sufficiently smooth exact solution χ, the global consistency conditions for (109) and (110) are, respectively,

$$B^{\mathrm{I}}_{\mathrm{GLS}}(w^h, \chi^h - \chi) = 0 \tag{114}$$

$$B^{\flat}_{\mathrm{GLS}}(w^h, \chi^h - \chi) = 0 \tag{115}$$

7.2. Energy estimates

LEMMA 7.1 (Total acoustic energy).

$$E_{\mathrm{f}}(w^h, w^h) = |\!|\!| w^h |\!|\!|_{\mathrm{f}}^2 \tag{116}$$

where

$$|\!|\!| w^h |\!|\!|_{\mathrm{f}}^2 := \mathscr{E}_{\mathrm{f}}(w^h(0^+)) + \sum_{n=1}^{N-1} \mathscr{E}_{\mathrm{f}}([\![w^h(t_n)]\!]) + \mathscr{E}_{\mathrm{f}}(w^h(T^-)) \tag{117}$$

and for linear acoustics, the total energy within the domain Ω_{f} is defined as in (30):

$$\mathscr{E}_{\mathrm{f}}(w) = \frac{1}{2} \|a\dot{w}\|_{\Omega_{\mathrm{f}}}^2 + \frac{1}{2} \|\nabla w\|_{\Omega_{\mathrm{f}}}^2 \tag{118}$$

This is the coercivity condition for the fluid.

PROOF.

$$\sum_{n=0}^{N-1} (\dot{w}^h, \ddot{w}^h)_{Q^{\mathrm{f}}_n} = \sum_{n=0}^{N-1} \int_{t_n}^{t_{n+1}} \frac{1}{2} \frac{\mathrm{d}}{\mathrm{d}t} \|a\dot{w}^h\|_{\Omega_{\mathrm{f}}}^2 \, \mathrm{d}t$$
$$= \frac{1}{2} \|a\dot{w}^h(T^-)\|_{\Omega_{\mathrm{f}}}^2 - \frac{1}{2} \|a\dot{w}^h(0^+)\|_{\Omega_{\mathrm{f}}}^2 + \frac{1}{2} \sum_{n=0}^{N-1} \{\|a\dot{w}^h(t_n^-)\|_{\Omega_{\mathrm{f}}}^2 - \|a\dot{w}^h(t_n^+)\|_{\Omega_{\mathrm{f}}}^2\} \tag{119}$$

Therefore,

$$E_2(w^h, w^h) = \frac{1}{2} \|a\dot{w}^h(T^-)\|_{\Omega_{\mathrm{f}}}^2 + \frac{1}{2} \|a\dot{w}^h(0^+)\|_{\Omega_{\mathrm{f}}}^2$$
$$+ \frac{1}{2} \sum_{n=1}^{N-1} \{\|a\dot{w}^h(t_n^+)\|_{\Omega_{\mathrm{f}}}^2 - 2(\dot{w}^h(t_n^+), a^2 \dot{w}^h(t_n^-))_{\Omega_{\mathrm{f}}} + \|a\dot{w}^h(t_n^-)\|_{\Omega_{\mathrm{f}}}^2\}$$
$$= \frac{1}{2} \|a\dot{w}^h(T^-)\|_{\Omega_{\mathrm{f}}}^2 + \frac{1}{2} \|a\dot{w}^h(0^+)\|_{\Omega_{\mathrm{f}}}^2 + \frac{1}{2} \sum_{n=1}^{N-1} \|a[\![\dot{w}^h(t_n)]\!]\|_{\Omega_{\mathrm{f}}}^2 \tag{120}$$

Similarly,

$$E_0(w^h, w^h) = \frac{1}{2}\|\nabla w^h(T^-)\|^2_{\Omega_f} + \frac{1}{2}\|\nabla w^h(0^+)\|^2_{\Omega_f} + \frac{1}{2}\sum_{n=1}^{N-1}\|[\![\nabla w^h(t_n)]\!]\|^2_{\Omega_f} \tag{121}$$

Combining (120) and (121) and using (101) completes the proof. □

LEMMA 7.2 (Radiation energy). For the exterior problem, assuming the non-reflecting boundary conditions satisfy condition (75), then

$$E_r(w^h, w^h) = |||w^h|||_r^2 \tag{122}$$

where

$$|||w^h|||_r^2 := \sum_{n=0}^{N-1} d_1(\dot{w}^h, \dot{w}^h)_{(\Gamma_\infty)_n} + \mathscr{E}_r(w^h(0^+)) + \sum_{n=0}^{N-1}\mathscr{E}_r([\![w^h(t_n)]\!]) + \mathscr{E}_r(w^h(T^-)) \tag{123}$$

and the operator $\mathscr{E}_r(\cdot)$ is defined as

$$\mathscr{E}_r(w) := \frac{1}{2}d_2(\dot{w}, \dot{w})_{\Gamma_\infty} + \frac{1}{2}d_0(w, w)_{\Gamma_\infty} \tag{124}$$

Eq. (123) represents a norm that is stronger than the radiation energy absorbed through the truncation boundary Γ_∞. For boundary operators up to second-order ($m = 2$):

$$\begin{aligned}\mathscr{R}(w) &:= \int_0^T\int_{\Gamma_\infty}\rho_0\dot{w}\mathbb{S}_m w\,d\Gamma\,dt \\ &= \mathscr{E}_r(w) + d_1(\dot{w}, \dot{w})_{\Gamma_\infty}\end{aligned} \tag{125}$$

PROOF. Proceeding as in Lemma 7.1,

$$\begin{aligned}\sum_{n=0}^{N-1} d_2(\dot{w}^h, \dot{w}^h)_{(\Gamma_\infty)_n} &= \frac{1}{2}d_2(\dot{w}^h(T^-), \dot{w}^h(T^-))_{\Gamma_\infty} - \frac{1}{2}d_2(\dot{w}^h(0^+), \dot{w}^h(0^+))_{\Gamma_\infty} \\ &\quad + \frac{1}{2}\sum_{n=1}^{N-1}\{d_2(\dot{w}^h(t_n^-), \dot{w}^h(t_n^-))_{\Gamma_\infty} - d_2(\dot{w}^h(t_n^+), \dot{w}^h(t_n^+))_{\Gamma_\infty}\}\end{aligned} \tag{126}$$

Therefore,

$$D_2(w^h, w^h) = \frac{1}{2}d_2(\dot{w}^h(T^-), \dot{w}^h(T^-))_{\Gamma_\infty} + \frac{1}{2}d_2(\dot{w}^h(0^+), \dot{w}^h(0^+))_{\Gamma_\infty} + \frac{1}{2}\sum_{n=0}^{N-1} d_2([\![\dot{w}^h(t_n)]\!], [\![\dot{w}^h(t_n)]\!])_{\Gamma_\infty} \tag{127}$$

Similarly,

$$D_0(w^h, w^h) = \frac{1}{2}d_0(w^h(T^-), w^h(T^-))_{\Gamma_\infty} + \frac{1}{2}d_0(w^h(0^+), w^h(0^+))_{\Gamma_\infty} + \frac{1}{2}\sum_{n=1}^{N-1} d_0([\![w^h(t_n)]\!], [\![w^h(t_n)]\!])_{\Gamma_\infty} \tag{128}$$

Combining (127), (128) and (102) completes the proof. □

LEMMA 7.3 (Total structural energy).

$$E_s(w^h, w^h) = |||w^h|||_s^2 \tag{129}$$

where

$$|||w^h|||_s^2 := \mathscr{E}_s(w^h(0^+)) + \sum_{n=1}^{N-1}\mathscr{E}_s([\![w^h(t_n)]\!]) + \mathscr{E}_s(w^h(T^-)) \tag{130}$$

and for elastodynamics, the total energy within the domain Ω_s is defined as in (29):

$$\mathscr{E}_s(w) = \frac{1}{2}(\dot{w}, \rho_s \dot{w})_{\Omega_s} + \frac{1}{2} a(w, w)_{\Omega_s} \tag{131}$$

This is the coercivity condition for the structure.

The proof of Lemma 7.3 follows the same steps taken to prove Lemma 7.1 and so is omitted (see also [6]).

The norm associated with the coupled fluid–structure system (109) and (110) is defined by:

$$\begin{aligned}
|||\psi^h|||^2 = {} & |||w^h|||_s^2 + |||w^h|||_f^2 + |||w^h|||_r^2 + \sum_{n=0}^{N-1} \{(\mathscr{L}_s w^h, \rho_s^{-1} \tau \mathscr{L}_s w^h)_{\tilde{Q}_n^s} \\
& + (\llbracket \sigma(\nabla w^h)(x) \rrbracket \cdot n, \rho_s^{-1} s \llbracket \sigma(\nabla w^h)(x) \rrbracket \cdot n)_{(\tilde{Y}_s)_n} + (\sigma(\nabla w^h) \cdot n, \rho_s^{-1} s \sigma(\nabla w^h) \cdot n)_{(Y_\sigma)_n} \\
& + (\mathscr{L}_1 \psi^h, \rho_s^{-1} s \mathscr{L}_1 \psi^h)_{(Y_s)_n} + \|c\tau^{1/2} \mathscr{L}_f w^h\|_{\tilde{Q}_n^f}^2 + \|cs^{1/2} \mathscr{L}_r w^h\|_{(\tilde{Y}_\infty)_n}^2 \\
& + \|cs^{1/2} \llbracket w_{,n}^h(x) \rrbracket\|_{(\tilde{Y}_f)_n}^2 + (\mathscr{L}_2 \psi^h, c^2 s \mathscr{L}_2 \psi^h)_{(Y_f)_n} \}
\end{aligned} \tag{132}$$

LEMMA 7.4 (Stability condition for the coupled system).

$$|||\psi^h|||^2 = B_{\mathrm{GLS}}^s(w^h, \psi^h) + B_{\mathrm{GLS}}^f(w^h, \psi^h) \tag{133}$$

PROOF. The proof follows directly from the superposition of (109) and (110),

$$\begin{aligned}
B_{\mathrm{GLS}}^s(w^h, \psi^h) + B_{\mathrm{GLS}}^f(w^h, \psi^h) = {} & E_s(w^h, w^h) - A(w^h, w^h) \\
& + E_f(w^h, w^h) + A(w^h, w^h) + E_r(w^h, w^h) \\
& + \sum_{n=0}^{N-1} \{B_{\mathrm{GLS}}^s(w^h, \psi)_n + B_{\mathrm{GLS}}^f(w^h, \psi)_n\}
\end{aligned} \tag{134}$$

Using the definitions in Lemmas 7.1, 7.2 and 7.3, and cancelling the coupling terms $A(\cdot, \cdot)$ completes the proof. The discontinuous Galerkin method ($\tau = 0, s = 0$) and/or ($\tau = 0, s = 0$), also satisfies a coercivity condition. □

REMARK. By the choice of displacement/velocity potential variables χ^h, weighting $\dot{\psi}^h$, and weakly enforcing the traction and kinematic interface boundary conditions across $\Gamma_\infty \times I_n$, then the coupling terms $A(\cdot, \cdot)$, cancel when the structure and the fluid variational equations are combined. Recall that an analogous result occurred in the construction of Lemma 3.1 for the continuum problem. This is the key result which allows for the establishment of a well-defined norm (132) for the coupled problem.

In the following, we establish the discrete counterpart to the energy identity obtained in Theorem 3.1 for the continuum problem.

THEOREM 7.1 (Energy estimate). In the absence of external loading, i.e. $f = 0$ and $\bar{t} = 0$, and assuming the radiation boundary operators satisfy (75), then at the end of a time interval the total structural energy, i.e. $\mathbb{E}(\chi^h(t_n^-))$, within the computational domain $\Omega = \Omega_s \cup \Omega_f$, plus the radiation energy absorbed through the artificial boundary Γ_∞, i.e. $\mathscr{R}(\phi^h(t_n^-))$, is bounded above by the initial energy in the system, i.e. $\mathbb{E}(\chi_0)$.

PROOF. With $f = 0$ and $\bar{t} = 0$,

$$\begin{aligned}
L_{\mathrm{GLS}}^s(u^h) + L_{\mathrm{GLS}}^f(\phi^h) &= (\dot{u}^h(0^+), \rho_s \dot{u}_0)_{\Omega_s} + a(u^h(0^+), u_0)_{\Omega_s} + (\dot{\phi}^h(0^+), a^2 \dot{\phi}_0)_{\Omega_f} + (\nabla \phi^h(0^+), \nabla \phi_0)_{\Omega_f} \\
&\leq |(\dot{u}^h(0^+), \rho_s \dot{u}_0)_{\Omega_s} + a(u^h(0^+), u_0)_{\Omega_s} \\
&\quad + (\dot{\phi}^h(0^+), a^2 \dot{\phi}_0)_{\Omega_f} + (\nabla \phi^h(0^+), \nabla \phi_0)_{\Omega_f}|
\end{aligned}$$

$$\leq \frac{1}{2}(\dot{u}^h(0^+), \rho_s \dot{u}^h(0^+))_{\Omega_s} + \frac{1}{2}(\dot{u}_0, \rho_s \dot{u}_0)_{\Omega_s} + \frac{1}{2}a(u^h(0^+), u^h(0^+))_{\Omega_s}$$
$$+ \frac{1}{2}a(u_0, u_0)_{\Omega_s} + \frac{1}{2}\|a\dot{\phi}^h(0^+)\|^2_{\Omega_f} + \frac{1}{2}\|a\dot{\phi}_0\|^2_{\Omega_f}$$
$$+ \frac{1}{2}\|\nabla\phi^h(0^+)\|^2_{\Omega_f} + \frac{1}{2}\|\nabla\phi_0\|^2_{\Omega_f}$$
$$= \mathscr{E}_s(u^h(0^+)) + \mathscr{E}_s(u_0) + \mathscr{E}_f(\phi^h(0^+)) + \mathscr{E}_f(\phi_0) \tag{135}$$

where $\mathscr{E}_s(u_0)$ and $\mathscr{E}_f(\phi_0)$ denote the initial total energy in the domains Ω_s and Ω_f, respectively. Adding (109) and (110), and using Lemma 7.4 and the definition of $|||\psi^h|||^2$ results in the energy estimate,

$$\mathscr{E}_s(u^h(T^-)) + \mathscr{E}_f(\phi^h(T^-)) + \mathscr{R}(\phi^h(T^-)) \leq \mathscr{E}_s(u_0) + \mathscr{E}_f(\phi_0) \tag{136}$$

Since T is arbitrary,

$$\mathbb{E}(\chi^h(t_n^-)) + \mathscr{R}(\phi^h(t_n^-)) \leq \mathbb{E}(\chi_0), \quad n = 0, 1, 2, \ldots, N-1 \tag{137}$$

where

$$\mathbb{E}(\chi^h(t_n^-)) := \mathscr{E}_s(u^h(t_n^-)) + \mathscr{E}_f(\phi^h(t_n^-)) \tag{138}$$

$$\mathbb{E}(\chi_0) := \mathscr{E}_s(u_0) + \mathscr{E}_f(\phi_0) \tag{139}$$

and $\mathscr{R}(\phi^h(t_n^-))$ is defined as in (125). Eq. (137) also holds for the time-discontinuous Galerkin method where $(\tau = 0, s = 0)$ and/or $(\tau = s = 0)$. □

This result is the algorithmic counterpart to the energy identity derived for the continuum problem and stated in Theorem 3.1. The energy decay inequality in (137) states that the total energy in the fluid–structure system, plus the energy absorbed through the radiation boundary, is always less than, or equal to the initial energy in the system, which implies that *the space–time formulation is unconditionally stable.*

COROLLARY 7.1 (Energy decay inequality for acoustics). For the uncoupled problem of linear acoustics, with zero sources, $f = 0$, and 'rigid' boundary conditions, i.e. $\dot{u}^h = \mathbf{0}$, then (137) reduces to

$$\mathscr{E}_f(\phi^h(t_n^-)) + \mathscr{R}(\phi^h(t_n^-)) \leq \mathscr{E}_f(\phi_0), \quad n = 0, 1, 2, \ldots, N-1 \tag{140}$$

As a specific example of the energy estimate (137), consider the first-order $\mathbb{S}_1$, non-reflecting boundary condition defined in (15). In this case the radiation energy (125) reduces to

$$\mathscr{R}(\phi^h) = \frac{1}{2}d_0(\phi^h, \phi^h)_{\Gamma_x} + d_1(\dot{\phi}^h, \dot{\phi}^h)_{\Gamma_x}$$
$$= \frac{1}{2}c_0\|\phi^h\|^2_{\Gamma_x} + c_1\|\dot{\phi}^h\|^2_{\Gamma_x} \tag{141}$$

where $c_0 = 1/R$ and $c_1 = 1/c$ are positive constants and (137) specializes to

$$\mathbb{E}(\chi^h(t_n^-)) + \frac{1}{2}c_0\|\phi^h\|^2_{\Gamma_x} + c_1\|\dot{\phi}^h\|^2_{\Gamma_x} \leq \mathbb{E}(\chi_0) \tag{142}$$

This result is the discrete counterpart to (45).

REMARK. The approach taken here for the coupling between the fluid and structure is applicable for either the interior or exterior problem. For the interior problem, no radiation boundaries are present and we have the energy estimate.

COROLLARY 7.2 (Energy decay inequality for the interior problem). For the interior (bounded) problem, (137) reduces to

$$\mathbb{E}(\chi^h(t_n^-)) \leq \mathbb{E}(\chi_0), \quad n = 0, 1, 2, \ldots, N-1 \tag{143}$$

This result establishes the unconditional stability of the formulation for the interior problem.

7.3. A priori error estimates for acoustics

Before stating the convergence rates for the coupled fluid–structure system, a priori error estimates for the simplified uncoupled problem of linear acoustics with 'rigid' boundary conditions are derived. To further simplify the analysis, non-reflecting boundary operators are restricted to the first-order $\mathbb{S}_1$ condition defined in (15). In this case, second-order time-derivatives do not appear in the radiation boundary condition and the boundary term $d_2(\cdot,\cdot)$ is omitted. The proof of convergence follows along the same lines as in [6], with the additional complication of including the non-reflecting boundary operators for the exterior problem.

For the acoustics problem with 'rigid' boundary conditions, (i.e. $\dot{\boldsymbol{u}}^h \cdot \boldsymbol{n} = 0$ on Γ_∞), the coupling operator $A(\boldsymbol{u}^h, w^h)$ vanishes and the norm associated with (109) reduces to

$$|||w^h|||^2 = |||w^h|||_{\mathrm{f}}^2 + |||w^h|||_{\mathrm{r}}^2 + \sum_{n=0}^{N-1} \{\|c\tau^{1/2}\mathscr{L}_{\mathrm{f}} w^h\|_{\dot{Q}_n^{\mathrm{f}}}^2 + \|cs^{1/2}\mathscr{L}_{\mathrm{r}} w^h\|_{(\tilde{\Gamma}_\infty)_n}^2 + \|cs^{1/2}[\![w^h_{,n}(\boldsymbol{x})]\!]\|_{(\tilde{\Gamma}_1)_n}^2 + \|cs^{1/2} w^h_{,n}\|_{(\Gamma_1)_n}^2\} \tag{144}$$

The coercivity condition for the uncoupled acoustics problem is then

$$|||w^h|||^2 = B^{\mathrm{f}}_{\mathrm{GLS}}(w^h, w^h) \tag{145}$$

where the right-hand side is defined by (109) with $A(\cdot,\cdot) = 0$. The consistency condition in this case is

$$B^{\mathrm{f}}_{\mathrm{GLS}}(w^h, e) = 0 \tag{146}$$

where $e = \phi^h - \phi$.

Let $\tilde{\phi}^h \in \mathscr{T}^h$ denote an interpolant of ϕ, and let $\eta = \tilde{\phi}^h - \phi$ denote the interpolation error. Then the solution error, $e = \phi^h - \phi$, can be split into the sum

$$e = e^h + \eta \tag{147}$$

where

$$e^h = \phi^h - \tilde{\phi}^h \in \mathscr{W}^h \tag{148}$$

is the difference between the finite element solution and the interpolant. An appropriate space–time mesh parameter is given by

$$h = \max\{c\,\Delta t, \Delta x\} \tag{149}$$

where c is the acoustic wave speed and Δx and Δt are maximum element diameters in space and time, respectively.

THEOREM 7.2 (Error estimates). Assume τ and s satisfy

$$c_1 h \leq \tau \leq c_2 h \tag{150}$$

$$c_3 \leq s \leq c_4 \tag{151}$$

where c_1, c_2, c_3 and c_4 are positive constants ($c_2 > c_1, c_4 > c_3$). Assuming the exact solution ϕ to the local acoustics problem with $\mathbb{S}_1$, is smooth in the sense that, $\phi \in H^{p+1}(Q_{\mathrm{f}})$ and assuming the interpolation error, η, satisfies the following estimates:

$$\sum_{n=0}^{N-1} d_1(\dot{\eta}, \dot{\eta})_{(\Gamma_\infty)_n} \leq c(\phi) h^{2p-1} \tag{152}$$

$$\sum_{n=0}^{N-1} \|a\tau^{-1/2}\dot{\eta}\|^2_{Q_n^t} \leq c(\phi)h^{2p-1} \tag{153}$$

$$\sum_{n=0}^{N-1} \|c\tau^{1/2}\mathscr{L}_t\eta\|^2_{\tilde{Q}_n^t} \leq c(\phi)h^{2p-1} \tag{154}$$

$$\sum_{n=0}^{N-1} \|as^{-1/2}\dot{\eta}\|^2_{(Y_\alpha)_n} \leq c(\phi)h^{2p-1} \tag{155}$$

$$\sum_{n=0}^{N-1} \|cs^{1/2}\mathscr{L}_x\eta\|^2_{(Y_\alpha)_n} \leq c(\phi)h^{2p-1} \tag{156}$$

$$\sum_{n=0}^{N-1} \|as^{-1/2}\dot{\eta}\|^2_{\tilde{Y}_n \cup (Y_1)_n} \leq c(\phi)h^{2p-1} \tag{157}$$

$$\sum_{n=0}^{N-1} \{\|cs^{1/2}[\![\eta_{,n}(x)]\!]\|^2_{\tilde{Y}_n} + \|cs^{1/2}\eta_{,n}\|_{(Y_1)_n}\} \leq c(\phi)h^{2p-1} \tag{158}$$

$$\mathscr{E}_t(\eta(T^-)) + \mathscr{E}_t(\eta(0^+)) + \sum_{n=1}^{N-1} \{\mathscr{E}_t(\eta(t_n^-)) + \mathscr{E}_t(\eta(t_n^+))\} \leq c(\phi)h^{2p-1} \tag{159}$$

$$d_0(\eta(T^-),\eta(T^-))_{\Gamma_\alpha} + d_0(\eta(0^+),\eta(0^+))_{\Gamma_\alpha} + \sum_{n=1}^{N-1} \{d_0(\eta(t_n^-),\eta(t_n^-))_{\Gamma_\alpha} + d_0(\eta(t_n^+),\eta(t_n^+))_{\Gamma_\alpha}\} \leq c(\phi)h^{2p-1} \tag{160}$$

where $c(\phi)$ is independent of the mesh parameter h, then

$$|||e|||^2 \leq c(\phi)h^{2p-1} \tag{161}$$

The following Lemmas aid in the proof of Theorem 7.2.

LEMMA 7.5.

$$E_2(e^h,\eta) = -\sum_{n=0}^{N-1} (\ddot{e}^h, a^2\dot{\eta})_{Q_n^t} - \sum_{n=1}^{N-1} ([\![\dot{e}^h(t_n)]\!], a^2\dot{\eta}(t_n^-))_{\Omega_t} + (\dot{e}^h(T^-), a^2\dot{\eta}(T^-))_{\Omega_t} \tag{162}$$

$$E_0(e^h,\eta) = -\sum_{n=0}^{N-1} (\nabla e^h, \nabla\dot{\eta})_{Q_n^t} - \sum_{n=1}^{N-1} ([\![\nabla e^h(t_n)]\!], \nabla\eta(t_n^-))_{\Omega_t} + (\nabla e^h(T^-), \nabla\eta(T^-))_{\Omega_t} \tag{163}$$

$$D_0(e^h,\eta) = -\sum_{n=0}^{N-1} d_0(e^h,\dot{\eta})_{(Y_\alpha)_n} - \sum_{n=1}^{N-1} d_0([\![e^h(t_n)]\!], \eta(t_n))_{\Gamma_\alpha} + d_0(e^h(T^-),\eta(T^-))_{\Gamma_\alpha} \tag{164}$$

Results (162)–(164) follow directly using definitions (104), (105) and (107), and from integration-by-parts in time. □

LEMMA 7.6.

$$\begin{aligned}(\ddot{e}^h, a^2\dot{\eta})_{Q_n^t} + (\nabla e^h, \nabla\dot{\eta})_{Q_n^t} + d_0(e^h,\dot{\eta})_{(Y_\alpha)_n} + d_1(\dot{e}^h,\dot{\eta})_{(Y_\alpha)_n} \\ = (\mathscr{L}_t e^h, \dot{\eta})_{\tilde{Q}_n^t} + (\mathscr{L}_x e^h, \dot{\eta})_{(Y_\alpha)_n} + ([\![e^h_{,n}(x)]\!], \dot{\eta})_{\tilde{Y}_n^t} + (e^h_{,n}, \dot{\eta})_{(Y_1)_n}\end{aligned} \tag{165}$$

PROOF. By integration-by-parts and the divergence theorem

$$(\nabla e^h, \nabla\dot{\eta})_{Q_n^t} = -(\nabla^2 e^h, \dot{\eta})_{\tilde{Q}_n^t} + (e^h_{,n}, \dot{\eta})_{(Y_\alpha)_n} + ([\![e^h_{,n}(x)]\!], \dot{\eta})_{\tilde{Y}_n^t} + (e^h_{,n}, \dot{\eta})_{(Y_1)_n} \tag{166}$$

Thus

$$(\ddot{e}^h, a^2\dot{\eta})_{Q_n^t} + (\nabla e^h, \nabla\dot{\eta})_{Q_n^t} + d_0(e^h, \dot{\eta})_{(\Gamma_s)_n} + d_1(\dot{e}^h, \dot{\eta})_{(\Gamma_s)_n}$$
$$= (a^2\ddot{e}^h - \nabla^2 e^h, \dot{\eta})_{\bar{Q}_n^t} + (e^h_{,n} + \mathbb{S}_1 e^h, \dot{\eta})_{(\Gamma_s)_n} + (\llbracket e^h_{,n}(x)\rrbracket, \dot{\eta})_{\bar{\Gamma}_n^t} + (e^h_{,n}, \dot{\eta})_{(\Gamma_t)_n} \tag{167}$$

where use is made of (69)–(71) with the first-order $m = 1$, non-reflecting boundary operator defined as in (15), i.e.

$$\mathbb{S}_1 e^h = \frac{1}{R}\, e^h + \frac{1}{c}\, \dot{e}^h \tag{168}$$

Employing the definitions (88) and (89) completes the proof. □

The following two inequalities are also needed.

$$\sum_{n=1}^{N-1} \{ -(\llbracket \dot{e}^h(t_n)\rrbracket, a^2\dot{\eta}(t_n^-))_{\Omega_t} - (\llbracket \nabla e^h(t_n)\rrbracket, \nabla\eta(t_n^-))_{\Omega_t}\} + (\dot{e}^h(T^-), a^2\dot{\eta}(T^-))_{\Omega_t} + (\nabla e^h(T^-), \nabla\eta(T^-))_{\Omega_t}$$
$$\leq \frac{1}{2}\left[\sum_{n=1}^{N-1} \{\mathscr{E}_t(\llbracket e^h(t_n)\rrbracket) + 4\mathscr{E}_t\{\eta(t_n^-))\} + \mathscr{E}_t(e^h(T^-)) + 4\mathscr{E}_t(\eta(T^-))\right] \tag{169}$$

Similarly,

$$-\sum_{n=1}^{N-1} d_0(\llbracket e^h(t_n)\rrbracket, \eta(t_n^-))_{\Gamma_s} + d_0(e^h(T^-), \eta(T^-))_{\Gamma_s}$$
$$\leq \frac{1}{2}\left[\sum_{n=1}^{N-1} \left\{ \frac{1}{2} d_0(\llbracket e^h(t_n)\rrbracket, \llbracket e^h(t_n)\rrbracket)_{\Gamma_s} + 2d_0(\eta(t_n^-), \eta(t_n^-))_{\Gamma_s} \right\} \right.$$
$$\left. + \frac{1}{2} d_0(e^h(T^-), e^h(T^-))_{\Gamma_s} + 2d_0(\eta(T^-), \eta(T^-))_{\Gamma_s} \right] \tag{170}$$

Results (169) and (170) follow directly from repeated use of the inequality

$$|(u, v)| \leq \frac{1}{2}\left(\frac{1}{\epsilon}\|u\|^2 + \epsilon\|v\|^2 \right), \quad \forall\, \epsilon > 0 \tag{171}$$

The proof of Theorem 7.2 proceeds as follows

$$|||e^h|||^2 = B^t_{\mathrm{GLS}}(e^h, e^h) \qquad \text{(by the coercivity condition, (145))}$$
$$= B^t_{\mathrm{GLS}}(e^h, e - \eta) \quad \text{(by (147))}$$
$$= -B^t_{\mathrm{GLS}}(e^h, \eta) \qquad \text{(by the consistency condition, (146))}$$
$$\leq |B^t_{\mathrm{GLS}}(e^h, \eta)|$$
$$= |E_2(e^h, \eta) + E_0(e^h, \eta) + D_1(e^h, \eta) + D_0(e^h, \eta)$$
$$+ \sum_{n=0}^{N-1} \{(\mathscr{L}_t e^h, c^2\tau\mathscr{L}_t\eta)_{\bar{Q}_n^t} + (\mathscr{L}_r e^h, c^2 s\mathscr{L}_r\eta)_{(\Gamma_s)_n}$$
$$+ (\llbracket e^h_{,n}(x)\rrbracket, c^2 s\llbracket \eta_{,n}(x)\rrbracket)_{\bar{\Gamma}_n^t} + (e^h_{,n}, c^2 s\eta_{,n})_{(\Gamma_t)_n}\}| \quad \text{(by definition of } B^t_{\mathrm{GLS}}\text{, (101)–(108))}$$
$$= \left| \sum_{n=0}^{N-1} \{ -(\mathscr{L}_t e^h, \dot{\eta})_{\bar{Q}_n^t} + (\mathscr{L}_t e^h, c^2\tau\mathscr{L}_t\eta)_{\bar{Q}_n^t} \right.$$
$$- (\mathscr{L}_r e^h, \dot{\eta})_{(\Gamma_s)_n} + (\mathscr{L}_r e^h, c^2 s\mathscr{L}_r\eta)_{(\Gamma_s)_n} + 2d_1(\dot{e}^h, \dot{\eta})_{(\Gamma_s)_n}$$
$$- (\llbracket e^h_{,n}(x)\rrbracket, \dot{\eta})_{\bar{\Gamma}_n^t} - (e^h_{,n}, \dot{\eta})_{(\Gamma_t)_n} + (\llbracket e^h_{,n}(x)\rrbracket, c^2 s\llbracket \eta_{,n}(x)\rrbracket)_{\bar{\Gamma}_n^t} + (e^h_{,n}, c^2 s\eta_{,n})_{(\Gamma_t)_n}\}$$
$$+ \sum_{n=1}^{N-1} \{ -(\llbracket \dot{e}^h(t_n)\rrbracket, a^2\dot{\eta}(t_n^-))_{\Omega_t} - (\llbracket \nabla e^h(t_n)\rrbracket, \nabla\eta(t_n^-))_{\Omega_t}\}$$
$$+ (\dot{e}^h(T^-), a^2\dot{\eta}(T^-))_{\Omega_t} + (\nabla e^h(T^-), \nabla\eta(T^-))_{\Omega_t}$$
$$\left. - \sum_{n=1}^{N-1} d_0(\llbracket e^h(t_n)\rrbracket, \eta(t_n^-))_{\Gamma_s} + d_0(e^h(T^-), \eta(T^-))_{\Gamma_s} \right| \quad \text{(by Lemmas 7.5 and 7.6)}$$

$$\leq \sum_{n=0}^{N-1} \Big\{ \frac{1}{4} \|c\tau^{1/2}\mathscr{L}_t e^h\|^2_{\tilde{Q}^t_n} + \|a\tau^{-1/2}\dot{\eta}\|^2_{\tilde{Q}^t_n} + \frac{1}{4} \|c\tau^{1/2}\mathscr{L}_t e^h\|^2_{\tilde{Q}^t_n} + \|c\tau^{1/2}\mathscr{L}_t \eta\|^2_{\tilde{Q}^t_n}$$
$$+ \frac{1}{4} \|cs^{1/2}\mathscr{L}_x e^h\|^2_{(Y_x)_n} + \|as^{-1/2}\dot{\eta}\|^2_{(Y_x)_n} + \frac{1}{4} \|cs^{1/2}\mathscr{L}_x e^h\|^2_{(Y_x)_n} + \|cs^{1/2}\mathscr{L}_x \eta\|^2_{(Y_x)_n}$$
$$+ \frac{1}{2} d_1(\dot{e}^h, \dot{e}^h)_{(Y_x)_n} + 2d_1(\dot{\eta}, \dot{\eta})_{(Y_x)_n} + \frac{1}{4} \|cs^{1/2}[\![e^h_{,x}(x)]\!]\|^2_{\tilde{Y}^t_n} + \|as^{-1/2}\dot{\eta}\|^2_{\tilde{Y}^t_n}$$
$$+ \frac{1}{4} \|cs^{1/2}e^h_{,n}\|^2_{(Y_t)_n} + \|as^{-1/2}\dot{\eta}\|^2_{(Y_t)_n} + \frac{1}{4} \|cs^{1/2}[\![e^h_{,n}(x)]\!]\|^2_{\tilde{Y}^t_n} + \|cs^{1/2}[\![\eta_{,n}(x)]\!]\|^2_{\tilde{Y}^t_n}$$
$$+ \frac{1}{4} \|cs^{1/2}e^h_{,n}\|^2_{(Y_t)_n} + \|cs^{1/2}\eta_{,n}\|^2_{(Y_t)_n} \Big\} + \frac{1}{2} \sum_{n=1}^{N-1} \{\mathscr{E}_t([\![e^h(t_n)]\!]) + 4\mathscr{E}_t(\eta(t_n^-))\}$$
$$+ \frac{1}{2} \mathscr{E}_t(e^h(T^-)) + 2\mathscr{E}_t(\eta(T^-)) + \frac{1}{4} \sum_{n=1}^{N-1} \{d_0([\![e^h(t_n)]\!], [\![e^h(t_n)]\!])_{\Gamma_x} + 4d_0(\eta(t_n^-), \eta(t_n^-))_{\Gamma_x}\}$$
$$+ \frac{1}{4} d_0(e^h(T^-), e^h(T^-))_{\Gamma_x} + 4d_0(\eta(T^-), \eta(T^-))_{\Gamma_x}$$

(by (171) and results (169) and (170))

The terms involving e^h may be subsumed by the left-hand side. The interpolation estimates (152)–(160) then yield

$$|||e^h|||^2 \leq c(\phi)h^{2p-1} \tag{172}$$

Likewise,

$$|||\eta|||^2 \leq c(\phi)h^{2p-1} \tag{173}$$

By the triangle inequality,

$$|||e|||^2 \leq 2|||e^h|||^2 + 2|||\eta|||^2 \leq c(\phi)h^{2p-1} \tag{174}$$

which completes the proof. □

This result indicates that the error as measured in the natural norm (145) for the discontinuous GLS solution to the exterior acoustics problem converges at the rate $(2p-1)/2$.

8. A simple model problem

To demonstrate the convergence and energy properties of the space–time finite element formulation, the response of a one-dimensional model problem in the semi-infinite interval $0 \leq x < \infty$ was calculated by introducing a truncation boundary $\Gamma_x = L$, and imposing an exact non-reflecting boundary condition. Consider the following initial/boundary-value problem,

$$\ddot{\phi} = c^2\phi_{,xx} \quad \text{for } x \in \Omega, t > 0 \tag{175}$$

$$\phi(0,t) = 0, \qquad \phi_{,x}(L,t) = -(1/c)\dot{\phi}(L,t) \tag{176}$$

$$\phi(x,0) = \phi_0(x), \qquad \dot{\phi}(x,0) = 0 \tag{177}$$

where $\Omega =]0, L[$ and the condition at $x = L$ in (176) is the exact 'plane-wave' non-reflecting boundary condition for this one-dimension problem. The initial pulse,

$$\phi_0(x) = \frac{1}{4}\left(1 - \cos\frac{2\pi}{\lambda}(x - x_0)\right)^2 \tag{178}$$

is positioned at the distance $x_0 = 2.4$ from the fixed end, with $\lambda = 0.8$, and the computational domain is taken as $\Omega =]0, 4[$, i.e. $L = 4$. The domain Ω is discretized uniformly with standard biquadratic

interpolations, $Q2$, in space–time, with 3×3 Gaussian quadrature used throughout. Quadratic interpolation in time is used to resolve the second-order temporal derivatives appearing in (60).

The exact solution is given by D'Alembert. Half of the initial pulse propagates with velocity $c = 1$, in each direction, i.e.

$$\phi(x,t) = \frac{1}{2}[\phi_0(\xi_+) + \phi_0(\xi_-)] \tag{179}$$

for $0 \leq \xi_+ \leq \lambda$ and $0 \leq \xi_- \leq \lambda$ where $\xi_+ = x - x_0 - ct$ and $\xi_- = x - x_0 + ct$. At time $t = 0.8$, the wave propagating to the right, $\phi_0(\xi_+)$, reaches the truncation boundary $\Gamma_\infty = L$, and at $t = 1.6$, this wave leaves Ω entirely. At time $t = 2.4$ the wave propagating to the left, $\phi_0(\xi_-)$, reaches the fixed end and is reflected back. At time $t = 7.2$, the reflected wave leaves Ω, resulting in a quiescent solution. The form of ϕ_0 is chosen such that the solution $\phi(x,t)$ has sufficient smoothness (continuity) for the interpolation estimates given in (152)–(160) to be valid. For ϕ_0 defined in (178), and quadratic space–time elements $p = 2$, the exact solution satisfies the requirement $\phi \in H^3$.

Fig. 3 shows the numerical solution using the time-discontinuous Galerkin Least-Squares algorithm at three representative times. Each space–time slab was discretized with a uniform mesh of 160 $Q2$ elements. The intrinsic time scale used for all computations is

$$\tau = \frac{\Delta t}{8\sqrt{1 + C^2}} \tag{180}$$

where $C = c\,\Delta t/\Delta x$ is the Courant number. The effect of the slowness parameter s, has little consequence on the solution to this problem, and as pointed out by Hulbert and Hughes [7], due to the complications involved with its assembly, this term is omitted in all the computations.

The energy properties of the exact solution are summarized in the following. The total energy within Ω is the sum of the kinetic and potential energies, i.e.

$$\mathscr{E}(\phi(t)) = \frac{1}{2}\|a\dot{\phi}\|_\Omega^2 + \frac{1}{2}\|\phi_{,x}\|_\Omega^2 \tag{181}$$

where

$$\|a\dot{\phi}\|_\Omega^2 = \int_0^L (a\dot{\phi}(x,t))^2\,dx$$

$$\|\phi_{,x}\|_\Omega^2 = \int_0^L (\phi_{,x}(x,t))^2\,dx$$

For the initial condition ϕ_0 given in (178), $\|a\dot{\phi}\|_\Omega^2 = \|\phi_{,x}\|_\Omega^2$ for $t \geq \lambda/2c$. In addition to the energy in Ω, the power flow, or rate of transfer of energy past the truncation boundary $\Gamma_\infty = L$, is

$$\frac{1}{c}(\dot{\phi}(L,t))^2 \geq 0 \tag{182}$$

and it can be shown that the total energy in Ω, plus the energy entering the exterior domain $x > L$, is conserved, i.e.

$$\mathscr{E}(\phi(t)) + \mathscr{R}(\phi(t)) = \mathscr{E}(\phi_0) \tag{183}$$

where the radiation energy defined in (125) is specialized in one dimension to

$$\mathscr{R}(\phi) = \frac{1}{c}\int_0^t (\dot{\phi}(L,\eta))^2\,d\eta \tag{184}$$

Fig. 4 shows the energy calculations for the time-discontinuous Galerkin Least-Squares formulation, with the Courant number set at $C = 1$. At $t = 0$, all the energy is potential, and as the initial pulse begins to propagate, energy is transformed from potential to kinetic. For $t \geq \lambda/2c = 0.4$, the initial pulse has completely separated into a lift and right wave, and the space–time finite element solution preserves the equality of the potential and kinetic energies, i.e. $\|a\dot{\phi}^h\|_\Omega^2 = \|\phi^h_{,x}\|_\Omega^2$. At $t = 0.8$, the right going wave reaches $\Gamma_\infty = L$, and the loss in total energy $\mathscr{E}(\phi^h)$ within Ω, is absorbed by the non-reflecting boundary

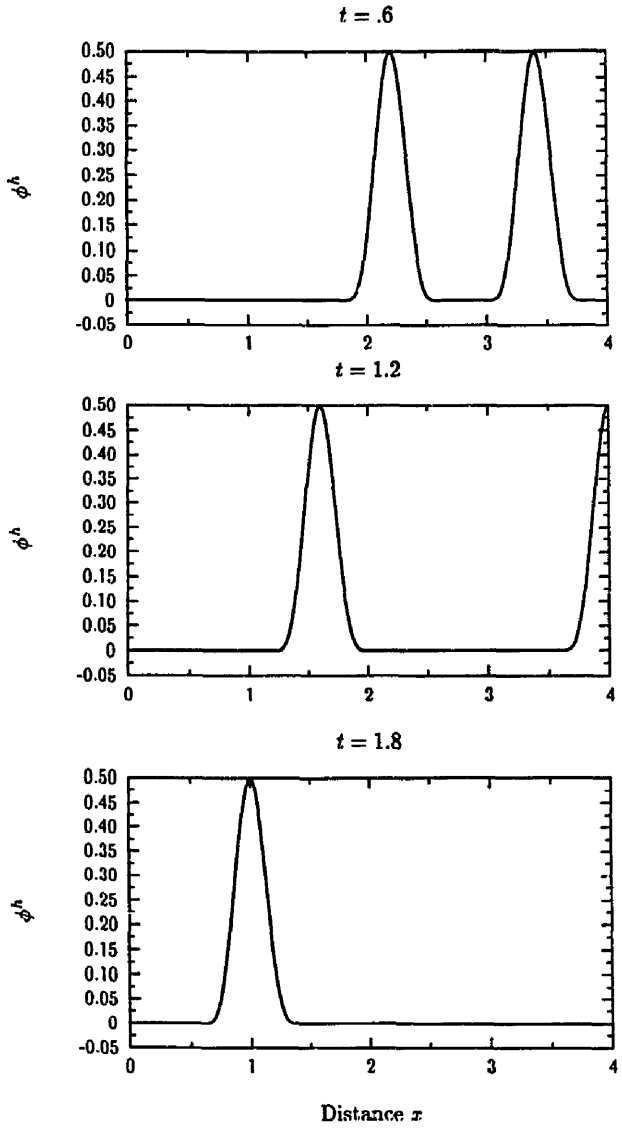

Fig. 3. One-dimension semi-infinite problem: Numerical solution using time-discontinuous GLS algorithm with 160 $Q2$ elements and a Courant number of $C = 1$. At time $t = 0.6$ two waves travel in opposite directions. At $t = 1.2$ the wave propagating to the right is absorbed by the non-reflecting boundary located at $x = 4$. At $t = 1.8$ only the left-going wave remains.

condition as measured by the radiation energy $\mathscr{R}(\phi^h)$. Results confirm that the Galerkin Least-Squares method is indeed dissipative, and matches the energy-decay inequality given in Theorem 7.1, i.e. the total energy plus the radiation energy is bounded above by the initial energy in the computational domain, i.e.

$$\mathscr{E}(\phi^h((t_n^-)) + \mathscr{R}(\phi^h(t_n^-)) \leq \mathscr{E}(\phi_0) \tag{185}$$

To study the numerical convergence, the response was calculated for the time interval $0 \leq t \leq T = 1.8$.

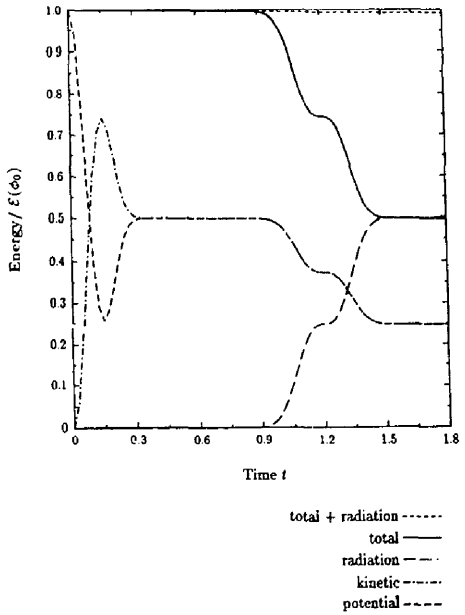

Fig. 4. Energy calculations using time-discontinuous Galerkin Least-Squares algorithm with 160 $Q2$ elements and Courant number $C = 1$. (Total energy = Kinetic energy + Potential energy.) Results confirm that the total energy plus the radiation energy is bounded above by the initial energy $\mathcal{E}(\phi_0)$.

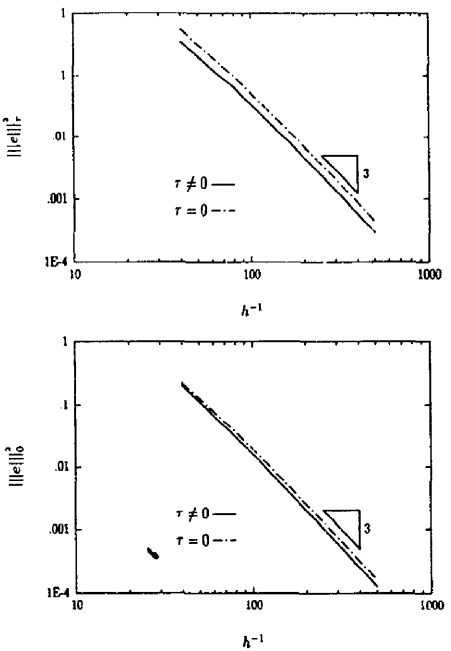

Fig. 5. Convergence of the numerical error for different formulations employing the $Q2$ element and $C = 1$; h is the length of the element. Results confirm the convergence rate $(2p - 1) = 3$ for $p = 2$.

The convergence rates for the time-discontinuous Galerkin and Galerkin Least-Squares formulations are shown in Fig. 5. Errors were measured in two different norms: $|||\cdot|||_\tau$ denotes the norm (144), with $s=0$, and $|||\cdot|||_0$ denotes the Galerkin norm, with $\tau=0$, $s=0$. Note that the convergence rates are identical for all formulations measured in both norms, and are the same as those predicted by Theorem 7.2. Results for this example show that the Galerkin formulation converges at the same rate as the GLS formulation, with slightly larger errors.

9. A priori error estimates for the coupled problem

In this section, error estimates are given for the coupled structural acoustics formulation. The convergence proof for the coupled fluid–structure problem follows the same basic steps as the uncoupled acoustics problem given in Section 7.3; further details are given in [27]. The results are stated for the $\mathbb{S}_1$ boundary condition only. Let $\P\boldsymbol{\chi}^h \in \mathcal{S}^h \times \mathcal{T}^h$ denote an interpolant of $\boldsymbol{\chi} := \{\boldsymbol{u}, \phi\}$. Then the error $\boldsymbol{E} = \boldsymbol{\chi}^h - \boldsymbol{\chi}$, can be written as:

$$\boldsymbol{E} = \boldsymbol{E}^h + \boldsymbol{H} \tag{186}$$

where

$$\boldsymbol{E}^h = (\boldsymbol{\chi}^h - \P\boldsymbol{\chi}^h) \in \mathcal{V}^h \times \mathcal{W}^h \tag{187}$$

$$\boldsymbol{H} = \P\boldsymbol{\chi}^h - \boldsymbol{\chi} \quad \text{(interpolation error)} \tag{188}$$

In components, $\boldsymbol{E} = \{\boldsymbol{e}, e\}$, $\boldsymbol{E}^h = \{\boldsymbol{e}^h, e^h\}$, and $\boldsymbol{H} = \{\boldsymbol{\eta}, \eta\}$ where $\boldsymbol{e} = \boldsymbol{u}^h - \boldsymbol{u}$ and $e = \phi^h - \phi$. An appropriate space–time mesh parameter for the structural domain Ω_s is given by $h_s = \max\{c_L \Delta t, \Delta x\}$ where c_L is the dilatational wave speed and Δx and Δt are maximum element diameters in space and time, respectively. For the fluid domain Ω_f, $h_f = \max\{c \Delta t, \Delta x\}$ where c is the acoustic wave speed.

Assuming τ and s satisfy the conditions given previously in (150) and (151). Similarly, assuming $\boldsymbol{\tau}$ and $\boldsymbol{s}$ satisfy,

$$c_1 h_s \leq \|\boldsymbol{\tau}\| \leq c_2 h_s \tag{189}$$

$$c_3 \leq \|\boldsymbol{s}\| \leq c_4 \tag{190}$$

where c_1, c_2, c_3 and c_4 are positive constants ($c_2 > c_1$, $c_4 > c_3$), and assuming $\boldsymbol{\chi} \in (H^{k+1}(Q_s))^d \times H^{p+1}(Q_f)$, together with standard interpolation estimates for $\boldsymbol{H}$, then it can be shown that the following estimate holds:

$$|||\boldsymbol{E}|||^2 \leq c(\boldsymbol{u}) h_s^{2k-1} + c(\phi) h_f^{2p-1} \tag{191}$$

where $c(\boldsymbol{u})$ and $c(\phi)$ are values that are independent of the mesh parameters, k and p are the order of the finite element interpolations for the structure and fluid, respectively, and $|||\cdot|||$ is the natural norm for the coupled system defined in (132). The proof of this a priori estimate follows the same basic steps as Theorem 7.2; details are given in [27]. This result indicates that the error for the coupled system is controlled by the convergence rates in both the structure and the fluid. In other words, for an accurate solution to the coupled fluid–structure problem, discretizations for both the structural domain and the fluid domain must be adequately resolved.

10. Closure

In this paper, a new space–time finite element formulation for transient structural acoustics involving the interaction of elastic structures vibrating in an unbounded acoustical fluid domain has been presented. The formulation is based on the time-discontinuous Galerkin method for second-order hyperbolic systems originally developed in the context of elastodynamics by Hughes and Hulbert [6]

and Hulbert and Hughes [7], extended here to time-dependent structural acoustics in exterior domains. A new space–time variational equation for the coupled problem is written in terms of structural displacement and acoustic velocity potential variables and includes the incorporation of high-order accurate non-reflecting boundary conditions. As a consequence of this choice of solution variables, the coupled space–time variational formulation for the fluid and structure gives rise to a positive norm for the coupled problem which enables us to prove the unconditional stability of the method.

For additional stability, and to prove convergence, least-squares operators based on local residuals of the Euler–Lagrange equations for the coupled system, including the non-reflecting boundary conditions, are included, giving rise to a Galerkin Least-Squares (GLS) space–time formulation. The least-squares operators are weighted by intrinsic time scale parameters, which may be designed to improve stability without degrading the accuracy of the underlying time-discontinuous Galerkin formulation. The GLS weighting parameters depend on element size and interpolation order. For the one-dimensional example presented, both Galerkin and GLS solutions converge. Additional numerical results (presented in [27, 33]), indicates that the Galerkin formulation should converge on general configurations as well, but from our error analysis, only GLS is guaranteed to converge.

Time-discontinuous Galerkin methods typically lead to systems of coupled equations which are larger than those emanating from standard semidiscrete methods. To approach economic competiveness with existing algorithms, the ability of space–time finite element methods to provide unified and simultaneous spatial and temporal adaptivity of the discretization must be exploited. Adaptive solution strategies are especially useful for applications to transient structural acoustics, in which both spatial and temporal enhancement can efficiently capture waves propagating along space–time characteristics. Recently, Johnson [34] and colleagues, have obtained some useful a posteriori error estimates based on the discontinuous Galerkin method for second-order hyperbolic equations. Having laid the foundations for the space–time finite element formulation for structural acoustics, research efforts are underway in the design and application of efficient and accurate local error indicators to drive adaptive and subcycling strategies for the transient structural acoustics problem incorporating high-order accurate non-reflecting boundaries.

In [27, 28] an extension of the time-discontinuous Galerkin space–time formulation presented in this paper is given where independent interpolation functions are used for both the acoustic velocity potential and its time derivative, i.e. the acoustic pressure. Hulbert [31] showed that asymptotic dissipation at high frequencies can be achieved by a multi-field formulation of this type, without the need for additional least-squares stabilization terms. An area of productive research is to compare the performance of the single-field and multi-field formulations in terms of both accuracy, as measured by numerical dispersion and high-frequency dissipation, and computational efficiency.

When space–time finite element methods are used to solve the structural acoustics problem in infinite domains, a fluid truncation boundary is introduced where radiation (non-reflecting) boundary conditions are applied to transmit outgoing waves. If accurate non-reflecting boundary conditions are used, fewer fluid elements are needed and considerable cost savings will result. Therefore, there is a need for the development of high-order accurate non-reflecting (absorbing) boundary conditions which eliminate or minimize reflection of outgoing waves and that also preserve the data structure of the space–time finite element method. In this paper, we have indicated how the time-discontinuous space–time finite element method provides a natural variational setting for the implementation of local in time non-reflecting boundary conditions. In the second part of this paper [25], a new sequence of high-order accurate and local in time non-reflecting boundary conditions based on an exact representation of the acoustic impedance are developed for solutions of the scalar wave equation in three space dimensions. Several numerical examples are given illustrating the high-order accuracy achieved by the implementation of these time-dependent absorbing boundary conditions in our space–time finite element formulation for the exterior structural acoustic problem.

Acknowledgments

This research was sponsored by the Office of Naval Research under Contract Numbers N00014-89-J-1951 and N00014-92-J-1774. The first author was also partially supported by an Achievement Rewards

for College Scientists (ARCS) fellowship. This support is gratefully acknowledged. We would also like to thank Thomas J.R. Hughes for inspiring our interest in space–time finite element technology, and Gregory M. Hulbert for access to the source code of his modified version of DLEARN.

References

[1] C. Johnson, U. Navert and J. Pitkaranta, Finite element methods for linear hyperbolic problems, Comput. Methods Appl. Mech. Engrg. 45 (1984) 285–312.
[2] C. Johnson, Numerical Solutions of Partial Differential Equations by the Finite Element Method (Cambridge University Press, New York, 1986).
[3] F. Shakib, T.J.R. Hughes and Z. Johan, A new finite element formulation for computational fluid dynamics: X. The compressible Euler and Navier–Stokes equations, Comput. Methods Appl. Mech. Engrg. 89 (1991) 141–219.
[4] G. Hauke and T.J.R. Hughes, A unified approach to compressible and incompressible flows, Comput. Methods Appl. Mech. Engrg. 113 (1994) 389–395.
[5] K. Jansen, Z. Johan and T.J.R. Hughes, Implementation of a one-equation turbulence model within a stabilized finite element formulation of a symmetric advective–diffusive system, Comput. Methods Appl. Mech. Engrg. 105 (1993) 405–433.
[6] T.J.R. Hughes and G.M. Hulbert, Space–time finite element methods for elastodynamics: Formulations and error estimates, Comput. Methods Appl. Mech. Engrg. 66 (1988) 339–363.
[7] G.M. Hulbert and T.J.R. Hughes, Space–time finite element methods for second-order hyperbolic equations, Comput. Methods Appl. Mech. Engrg. 84 (1990) 327–348.
[8] T.J.R. Hughes, L.P. Franca and G.M. Hilbert, A new finite element formulation for computational fluid dynamics: VIII. The Galerkin least squares method for advective–diffusive equations, Comput. Methods Appl. Mech. Engrg. 73 (1989) 173–189.
[9] I. Harari and T.J.R. Hughes, Finite element methods for Helmholtz equation in an exterior domain: Model problems, Comput. Methods Appl. Mech. Engrg. 87 (1991) 59–96.
[10] I. Harari and T.J.R. Hughes, Galerkin/least-squares finite element methods for the reduced wave equation with non-reflecting boundary conditions in unbounded domains, Comput. Methods Appl. Mech. Engrg. 98 (1992) 411–454.
[11] L.L. Thompson and P.M. Pinsky, A multi-dimensional Galerkin/Least-Squares finite element method for time-harmonic wave propagaton, in: R. Kleinman et al., ed., Second Int. Conf. on Mathematical and Numerical Aspects of Wave Propagation, Chapter 47 (SIAM, 1993) 444–451.
[12] L.L. Thompson and P.M. Pinsky, A Galerkin/least-squares finite element method for the two-dimensional Helmholtz equation, Int. J. Numer. Methods Engrg. 38 (1985) 371–397.
[13] I. Harari and T.J.R. Hughes, Stabilized finite element methods for steady advection–diffusion with production, Comput. Methods Appl. Mech. Engrg. 115 (1994) 165–191.
[14] G.C. Huang, G.C. Everstine and Y.F. Wang, Retarded potential techniques for the analysis of submerged structures impinged by weak shock waves, in: T. Belytschko and T.L. Geers, eds., Computational Methods for Fluid–Structure Interaction Problems, Vol. AMD 26 (ASME, New York, 1977) 83–93.
[15] H.C. Neilson, G.C. Everstine and Y.F. Wang, Transient response of a submerged fluid-coupled double-walled shell structure to a pressure pulse, J. Acoust. Soc. Am. 70 (1981) 1776–1782.
[16] Y.P. Lu, The application of retarded potential techniques to submerged dynamic structural systems, in: R.P. Shaw and W. Pilkey, eds., Proc. 2nd Int. Symposium Innovative Numerical Analysis for the Applied Engineering Sciences (1980) 59–68.
[17] P.M. Pinsky and N.N. Abboud, Finite element solution of the transient exterior structural acoustics problem based on the use of radially asymptotic boundary operators, Comput. Methods Appl. Mech. Engrg. 85 (1991) 311–348.
[18] P.M. Pinsky, L.L. Thompson and N.N. Abboud, Local high-order radiation boundary conditions for the two-dimensional time-dependent structural acoustics problem, J. Acoust. Soc. Am. 91(3) (1992) 1320–1335.
[19] A. Safjan, L. Demkowicz and J.T. Oden, Adaptive finite element methods for hyperbolic systems with applications to acoustics, Int. J. Numer. Methods Engrg. 32 (1991) 677–707.
[20] N.M. Newmark, A method of computation for structural dynamics, J. Engrg. Mech. Div., ASCE (1959) 67–94.
[21] H.M. Hilber, T.J.R. Hughes and R.L. Taylor, Improved numerical dissipation for time integration algorithms in structural dynamics, Earthquake Engrg. Struct. Dynam. 5 (1977) 283–292.
[22] E. Zauderer, Partial Differential Equations of Applied Mathematics, 2nd edition (Wiley-Interscience, New York, 1989).
[23] T.J.R. Hughes, Recent progress in the development and understanding of SUPG methods with special reference to the compressible Euler and Navier–Stokes equations, Int. J. Numer. Methods Fluids 7 (1987) 1261–1275.
[24] O.C. Zienkiewicz and P. Bettess, Fluid–structure dynamic interaction and wave forces: An introduction to numerical treatment, Int. J. Numer. Methods Engrg. 13 (1978) 1–16.
[25] L.L. Thompson and P.M. Pinsky, A space–time finite element method for structural acoustics in infinite domains, Part 2: Exact time-dependent non-reflecting boundary conditions, Comput. Methods Appl. Mech. Engrg. 132 (1996) 229–258.
[26] J. Lighthill, Waves in Fluids (Cambridge University Press, New York, 1978).
[27] L.L. Thompson, Design and analysis of space–time and Galerkin/least-squares finite element methods for fluid–structure interaction in exterior domains, Ph.D. Dissertation, April 1994, Stanford University, Stanford, CA, 1994.

[28] L.L. Thompson, A multi-field space–time finite element method for structural acoustics, Proc.: Symposium on Acoustics of Submerged Structures and Transduction Systems, ASME 15th Biennial Conference on Mechanical Vibration and Noise, Sept. 17–21, 1995, Boston, MA, 1995.

[29] D. Givoli and J.B. Keller, Special finite elements for use with high-order boundary conditions, Comput. Methods Appl. Mech. Engrg. 119 (1994) 119–213.

[30] F. Shakib and T.J.R. Hughes A new finite element formulation for computational fluid dynamics: IX. Fourier analysis of space–time Galerkin/least-squares algorithms. Comput. Methods Appl. Mech. Engrg. 87 (1991) 35–58.

[31] G.M. Hulbert, Space–time finite element methods for second-order hyperbolic equations, Ph.D. Dissertation, Stanford University, Stanford, CA. 1989.

[32] G.M. Hulbert, Discontinuity-capturing operators for elastodynamics. Comput. Methods Appl. Mech. Engrg. 96 (1992) 409–426.

[33] L.L. Thompson and P.M. Pinsky, A space–time finite element method for the exterior structural acoustics problem: Time-dependent radiation boundary conditions in two space dimensions, Int. J. Numer. Methods Engrg., in press.

[34] C. Johnson, Discontinuous Galerkin finite element methods for second-order hyperbolic problems, Comput. Methods Appl. Mech. Engrg. 107 (1993) 117–129.